Carbonate crusts have been recovered on the slopes of volcanic islands using remotely operated vehicles

Crusts consist of mixtures of volcaniclastic and biogenic fragments cemented together by calcite in various forms

Crusts are attributed to seawater circulating within the surficial sediment, in some cases mixing with hydrothermal fluids based on isotopic analyses

Crusts provide increased stability of submarine slops by armoring surficial sediments

Carbonate crusts around volcanic islands and their significance

Maurice E. Tucker[1], Steven N. Carey[2], R. Stephen J. Sparks[1], Adam Stinton[3,4], Melanie Leng[5], Laura Robinson[1], Tao Li[1,6], Jamie Lewis[1], Laura Cotton[1,7]

1. School of Earth Sciences, University of Bristol, Bristol BS8 1RJ, UK
2. Graduate School of Oceanography, University of Rhode Island, Narragansett, R.I. 02882
3. Montserrat Volcano Observatory, PO Box 316, Fleming, MSR 1110, Montserrat
4. Seismic Research Centre, The University of the West Indies, St Augustine, Trinidad and Tobago
5. British Geological Survey, Keyworth, Nottingham NG12 5GG, UK and School of Biosciences, University of Nottingham, Sutton Bonington Campus, Loughborough LE12 5RD, UK
6. Department of Earth and Planetary Sciences, Nanjing University, 163 Xianlin Road, Nanjing 210023, China
7. School of Earth & Environmental Sciences, University of Portsmouth, Burnaby Building, Burnaby Road, Portsmouth PO1 3QL, UK

ABSTRACT

Extensive carbonate crusts discovered forming on the slopes of seamounts in many parts of the world's oceans are providing extra stability to the volcanic edifices. These crusts are composed of mixtures of volcaniclastic debris and bioclastic material, in most cases cemented by calcite, in the form of isopachous coatings around grains and pore-filling spar. Such crusts, which have been collected by remotely-operated vehicle (ROV), are described here from moderate-depth to deeper-water slopes (200 – 1000 m) around the volcanic island of Montserrat in the Caribbean, and from the nearby Kick'em Jenny submarine volcano off Grenada. Radiogenic $^{87}Sr/^{86}Sr$ isotope ratios from the carbonates give an indication of age but also demonstrate that some samples have been altered by hydrothermal-volcanic processes, as shown by ages much older than expected. Such alteration is also supported by carbon and oxygen isotope ($\delta^{13}C$ and $\delta^{18}O$) ratios, although most samples have typical marine values. In many cases $\delta^{18}O$ is usually a little more positive than expected from modern shallow-water carbonates, likely reflecting cooler water at the depth of lithification. Just one sample, from Kick'em Jenny, has very negative $\delta^{13}C$ (-42 ‰) indicating methanogenesis. Crusts are also reported here from the Mediterranean Sea, with an example described from Kolumbo, northeast of the Santorini volcanic complex in the Hellenic subduction zone, that are similar in many respects to those from the Caribbean. Typically, the biota of the crusts consists of calcareous red algae (commonly encrusting volcanic clasts), benthic (also encrusting) and planktic foraminifera, subordinate serpulids, bivalves, pteropods and heteropods, and rare deeper-water corals. In addition, there is evidence for the former presence of microbes from the occurrence of calcified filaments and peloids in intragranular cavities. Several generations of sponge borings are usually present as well as calcite cement. The carbonate crusts are attributed to seawater circulating within the surficial sediment, in some cases mixing with hydrothermal fluid. The significance of these crusts is in stabilising seamounts, enabling their

slopes to avoid frequent collapse, dissection and readjustment, but when failure does occur, larger-scale submarine landslides involving coherent slabs are more likely.

Keywords: Seamounts, Montserrat, hardgrounds, carbonate crusts, slope crusts,

1. Introduction

Volcanic islands are favourable environments for the formation of carbonate sediment. Much attention has focussed on the formation of coral islands and atolls by the subsidence of volcanic islands following on from Darwin's seminal work (Darwin, 1874; Stoddart, 1976). Coral reefs surround volcanic islands and protect them from erosion by waves and storms. They are generated by biological activity but cementation is also involved due to interaction with carbonate-saturated fluids, notably seawater. We have discovered extensive carbonate-cemented crusts that mantle and armour the deeper flanks of volcanic islands and seamounts as submarine hardgrounds to water depths of several hundred metres. The hardgrounds form by cementation of volcaniclastic and bioclastic deposits that drape seamount slopes. Although hardgrounds are relatively common in shallow-water successions throughout the geological record, and relatively rare in deeper-water facies (Christie et al., 2015), the term "hardground" was first introduced by Murray and Renard (1891) as a descriptive term for rocky seafloors in the deep-sea discovered during the voyage of HMS Challenger in 1872-6. 'Classic' modern-Quaternary shallow-water hardgrounds are well-documented from carbonate-dominated locations such as the Bahamas and Arabian Gulf (e.g. Shinn, 1968; Dravis, 1978) and deeper-water ones occur there on slopes too (e.g. Schlager and James, 1978; Malone et al., 2001), as well as in the Mediterranean (Allouc, 1990; Aghib et al., 1991) and on cold-water mound structures, such as Porcupine Bank, in the NE Atlantic (Noé et al., 2006; van der Land et al., 2010). There are, however, fewer reports of carbonate crusts on the

slopes of seamounts and volcanic ridges, apart from some documented from the Mid-Atlantic Ridge (Thompson et al., 1968; Schroeder et al., 2002), the Mediterranean (McKenzie and Bernoulli, 1982) and Red Sea (e.g., Milliman, 1974). Several Quaternary hardgrounds have been related to sea-level and climate changes (see reviews of van der Kooij et al., 2010 and Christ et al., 2015).

Exploration of the submarine flanks of active volcanoes and volcanic seamounts during expeditions of the EV *Nautilus* has revealed common limestone crusts and hardgrounds covering their submarine slopes. These crusts typically consist of volcanogenic clastic and biogenic material cemented by calcite coating the slopes and extending to water depths of several hundred metres. They can be several tens of centimetres to a few metres thick and form distinctive slabs when fractured. They have been observed at the Soufrière Hills Volcano, Montserrat in the Eastern Caribbean, and around several seamounts and young submarine volcanoes in the Mediterranean and in the Galapagos Islands, all of which have been sampled. To our knowledge such carbonate crusts have not been widely recognised or described. However, they may be significant from several perspectives. First, they represent a new location of limestone deposition in the world's oceans. Second, the hardgrounds act to protect the submarine flanks of volcanic islands and seamounts from erosion and collapse and they may inhibit submarine intrusion of seawater into the interior of such volcanic edifices. In addition, they also form important hard substrates for the development of benthic biological communities.

This study focuses on the development of limestone crusts with a case study of the Soufrière Hills Volcano (SHV), Montserrat, together with descriptions of occurrences on other seamounts, in the southern Lesser Antilles (Kick'em Jenny submarine volcano) and, as a Mediterranean example, the Kolumbo seamounts from the Hellenic Arc in the Aegean Sea. We also note limestones sampled on Montserrat in geothermal boreholes and as clasts in

112 debris-avalanche deposits since they are pertinent to understanding the role of hydrothermal
113 and ground-water systems in forming the limestone crusts. The origin of the seamount-slope
114 limestones is elucidated through petrography, geochronology and isotope geochemical
115 studies. Important questions to be addressed include: what are the relative roles of inorganic
116 versus organic processes in the formation of the crusts; what are their rates of formation, and
117 what environmental factors such as water depth, temperature and fluid-flow related to
118 hydrothermal systems, are important controlling factors in their occurrence.
119

120 ## 2. Geological Settings

121 *2.1 The Soufrière Hills Volcano, Montserrat*

122 Montserrat is a predominantly andesitic volcanic island in the eastern Caribbean that is
123 elevated to a height of almost 2 km above the surrounding seafloor from water depths of 800
124 to 1000 m. The island comprises four volcanic centres (Fig. 1) which become younger from
125 north to south (Rea, 1974; Harford et al., 2002; Coussens et al., 2017; Hatter et al., 2018).
126 These centres are the Silver Hills (2.17 to 1.03 Ma), Centre Hills (1.14 to 0.38 Ma), South
127 Soufrière Hills (0.14 to 0.09 Ma) and the Soufrière Hills Volcano (SHV, 0.45 Ma to present).
128 The major eruption of the SHV between 1995-2010 (Kokelaar, 2002; Wadge et al., 2014) has
129 resulted in Montserrat being one of the most intensively studied island-arc volcanoes in the
130 World. A striking feature of the island morphology is the development of a moderate-depth
131 carbonate shelf (~ 120 to 140 m depth) that becomes wider to the north / northeast of the
132 island (figure 4 in Le Friant et al., 2004).
133 There are important tectonic structures in and around Montserrat. The island has developed at
134 a major offset in a regional transtensional fault zone (Feuillet et al., 2010). To the SE of
135 Montserrat, the Bouillante-Montserrat Fault Zone (Fig. 1) bounds a major half-graben to the
136 east (Watt et al., 2012). The Havers-Montserrat fault system lies to the NW of Montserrat.

137 The same fault zone, known as the Belham Valley fault, extends across the island between
138 the SHV and Centre Hills along a WNW-ESE trend. The Belham Valley fault is a complex
139 zone of deformation with localised uplift of the St George's and Garibaldi Hills. Lava domes,
140 fumaroles and hot springs of the SHV are elongated along the fault zone (Wadge et al.,
141 2014). A major geothermal field is centred on the Belham Valley and St George's Hill to the
142 NW of the SHV (Ryan et al., 2013). Seismic sections across the submarine fault-zone
143 (Kenedi et al., 2010) show it is a major listric system downthrown to the NNE with multiple
144 minor faulting across the footwall side with localised uplift in the hanging wall.
145
146 *2.2 Kick'em Jenny volcanic field*
147 Kick'em Jenny submarine volcano (KeJ) is located just 7.5 km north of the island of Grenada
148 in the southern Lesser Antilles (KeJ, Fig. 2). The first detailed bathymetric survey of the
149 volcano in 1972 revealed a 1300 m high conical structure, constructed on the western flank of
150 the arc with a summit crater at 190 m water-depth (Sigurdsson and Shepherd, 1974). Recent
151 SEABEAM mapping of the volcano has shown that the summit cone and crater actually lie
152 within a much larger arcuate collapse structure that opens to the west (Sigurdsson et al.,
153 2006). A debris avalanche deposit associated with formation of the horseshoe-shaped
154 collapse structure extends 17 km downslope into the back-arc Grenada Basin (Lindsay et al.,
155 2005; Dondin et al., 2012) with chemosynthetic cold seeps at the distal end (Carey et al.,
156 2014a). KeJ has erupted at least 12 times since 1939 and is currently the most active volcano
157 in the West Indies (Devas, 1974; Lindsay et al., 2005). Some of the eruptions produce surface
158 disturbances, subaerial plumes and minor tsunamis, whereas others have been detected only
159 by T-phase seismic signals (Shepherd and Robson, 1967; Lindsay et al., 2005). Recent
160 multibeam mapping and remotely-operated vehicle explorations of the area have revealed the
161 presence of several other small volcanic centres just to the east and southeast of KeJ (Carey et

al., 2015). The slopes of these centres, lying at about 200 metres water depth and apparently not recently active, exhibit common outcrops of carbonate crusts similar to those seen off the coast of Montserrat.

2.3 Kolumbo Submarine Volcanic Line

The seafloor northeast of Santorini volcano in Greece consists of a small, elongate rifted basin that has been the site of recent submarine volcanism (Kolumbo, Fig. 2). This area lies within the Cyclades back-arc region of the present-day Hellenic subduction zone where the seafloor of the eastern Mediterranean Sea is descending beneath the Aegean microplate. The Cycladic region and the Aegean Sea as a whole are known to be regions of south-easterly back-arc extension and thinning of continental crust. Nineteen submarine volcanic cones occur within this small rift zone, the largest of these being Kolumbo which last erupted explosively in 1650 AD, causing significant damage and fatalities on the nearby island of Santorini (Carey et al., 2011; Nomikou et al., 2012). Water depths of the submarine cones range from 18 to 450 metres. In general, the domes and craters northeast of Kolumbo are sediment covered and show little evidence of recent volcanic activity. Outcrops of volcanic rock can be found in the crater walls and slopes of some of the cones, but they typically consist of volcanic fragments of pumice and lava, along with some bioclastic material, cemented by calcite, indicative of the lack of recent eruptions.

3. Methods and Samples

Multibeam mapping and remotely-operated vehicle (ROV) explorations of the submarine flanks of Montserrat, Kick'em Jenny and the Kolumbo seamount chain in the Mediterranean enabled submarine hardground occurrences to be imaged and sampled (Carey et al., 2011; Carey et al., 2014a,b; Watt et al., 2015; Carey et al., 2015). In addition to *in-situ* samples in

187 the submarine environment, limestones have been sampled from three other settings on and
188 around Montserrat. The first is from outcrops of submarine volcaniclastic sediment with thin
189 (1-2 m thick) limestones on land at Roche's Bluff on the southeastern flank of Montserrat; a
190 volcanic clast here has an $^{40}Ar/^{39}Ar$ age of 1.02 Ma (Harford et al., 2002). Second,
191 geothermal boreholes in the Belham Valley have recovered limestones interbedded with
192 volcanics and intrusives in continuous core and in cuttings to depths of 2.3 km. And finally,
193 Holocene offshore debris-avalanche deposits contain clasts of shallow-water coralgal
194 limestone that have been transported into deeper water. Locations, water depths and brief
195 descriptions of the samples are given in Table 1.
196 All limestone samples, including those from the geothermal borehole and Roche's
197 Bluff outcrops, have been examined in thin-section. For stable isotope analysis of bulk
198 carbonate the sample material was ground in agate and 10 mg of carbonate powder was
199 reacted with anhydrous phosphoric acid in vacuo for 72 hours at a constant 25°C (Ca and Mg
200 carbonates including dolomite should react within this time) at the British Geological Survey
201 (BGS). The CO_2 liberated was separated from water vapour under vacuum and collected for
202 analysis. Measurements were made on a VG Optima mass spectrometer at BGS Keyworth,
203 UK. Overall analytical reproducibility for these samples is normally better than 0.2‰ for δ
204 ^{13}C and $\delta^{18}O$ (2σ). Isotope values ($\delta^{13}C$, $\delta^{18}O$) are reported as per mil (‰) deviations of the
205 isotopic ratios ($^{13}C/^{12}C$, $^{18}O/^{16}O$) calculated to the VPDB scale using a within-run laboratory
206 standard calibrated against NBS standards (Table 2).
207 Samples selected for strontium isotope seawater-age determinations were measured in the
208 Bristol Isotope Group facility at the University of Bristol. Following the protocol described in
209 Lewis et al. (2014), samples were dissolved in high purity acids and Sr separated using Sr
210 Spec resin (Horwitz et al., 1992). Samples were loaded on to single rhenium filaments with a
211 $TaCl_5$ activator (Birck, 1986) and Sr isotope ratios were measured using a Thermo-Finnigan

212 Triton thermal ionization mass spectrometer. Samples were measured using a multi-dynamic
213 'triple-jump' method (Thirlwall, 1991; Avanzinelli et al., 2004) of 200 cycles with a 4.194 s
214 integration time per cycle. Instrumental mass bias was corrected using an exponential mass
215 bias law and an $^{86}Sr/^{88}Sr$ of 0.1194 (Nier, 1938; Russell et al., 1978); ^{87}Rb is corrected by
216 monitoring ^{85}Rb and using an $^{85}Rb/^{87}Rb$ of 2.59265 (Steiger and Jäger, 1977). Long-term
217 reproducibility of $^{87}Sr/^{86}Sr$ for NIST SRM 987 processed through column chemistry is
218 0.710247 ± 0.00001 (2 SD, n = 58). Results are given in Table 3.
219
220 **4. Results**
221 *4.1 Petrography of Carbonate Crusts*
222 *4.1.1 Montserrat Submarine Slope Limestones*
223 Multibeam images of the western and south-western flanks of the SHV are shown in Fig. 3. A
224 limestone crust occurs as a continuous layer across the submarine surface to water depths of
225 several hundred metres, as observed and videoed by the ROV. The crust shows abrupt
226 boundaries where large slabs have broken off and detached, indicating mass wasting. Figures
227 4a and 5a show images of limestone slabs where they have been locally disrupted and tilted,
228 revealing their internal texture and lithology. The limestone crusts are typically made of
229 volcaniclastic material (boulder to silt grade), containing variable amounts of bioclastic
230 debris cemented by carbonate. There are also crusts largely composed of carbonate skeletal
231 debris with subsidiary volcanic clasts. These are strongly lithified rocks and contrast with the
232 unconsolidated and uncemented volcaniclastic deposits that form when lahars and pyroclastic
233 flows enter the ocean from the island (Le Friant et al., 2009; Trofimovs et al., 2012).
234 Samples of cemented slope limestone were collected by ROV from the nearshore area to the
235 SW of Montserrat. Two samples were located some 1-2 km from the shoreline (Fig. 3), at
236 188 m water depth (NA037-029) and 292 m (NA037-033). Both came from seafloor

exposures of disrupted limestone crust (Figs. 4 and 5). Two other limestone samples were located about 8 km from the shoreline (Figs. 6 and 7) and are associated with the debris avalanche known as deposit 5 (Le Friant et al., 2004), formed between 8 and 12 kyr (Cassidy et al., 2013) due to collapse of the shallow shelf platform. Sample NA037-025 comes from 806 m water depth and NA037-026 from 823 m.

Sample NA037-029 is a bioclastic volcanic-grain pack-grainstone with some pebble-sized volcanic clasts (Fig. 4a, b). Some granules-pebbles are coated by calcareous red algae (giving rhodoliths)(Fig. 4b); the sandy (< 2 mm) sediment consists of fragments of red and green calcareous algae (including *Halimeda*), foraminifera (several *Amphistegina*), bivalve, serpulid and echinoid. The sediment is moderately-well sorted with some larger coated grains. There are sponge borings in shells (Fig. 4c), filled with sediment, but these borings also penetrate the sediment, indicating an earlier phase of cementation. The micritic sediment contains diffuse peloids, and possible filaments, probably of microbial origin. In areas of intergranular pores and cavities, a fibrous-bladed isopachous calcite fringe occurs around grains (Fig. 4d). This rock was likely deposited from a sediment gravity flow or landslide and has been cemented *in situ* by a micritic and fibrous calcite cement to form a hardground.

Sample NA037-033 is also a true hardground from synsedimentary cementation of the submarine slope (Fig. 5a). It is a bioclastic volcaniclastic grainstone (Figure 5b), with larger clasts up to several cm, consisting of numerous shallow-water bioclasts: foraminifera (*Amphistegina*, *Peneroplis*, miliolinids), bivalves, gastropods, echinoids, calcareous algae – both red and green (*Halimeda*), and volcanic grains coated with calcareous red algae, serpulids and encrusting foraminifera (Figs. 5b-d). Planktic gastropods (pteropods and heteropods) are present as well as planktic foraminifera. Peloids, probably microbial, occur within cavities in a geopetal arrangement (Fig. 5d). The main cement between grains consists

of either an isopachous bladed calcite fringe or an isopachous micritic fringe (Figs. 5e, f). Within gastropods there are acicular aragonite cements, syntaxial upon the shell. There is still much empty pore space. This deposit is interpreted as resedimented, consisting of a mixture of volcanic crystals and clasts and shallow-water skeletal debris. However, there is also a planktic component indicating some mixing with pelagic sediment during slope transport.

Sample NA037-025 is a loose piece of cemented sand (Fig. 6a) from a deep-water slope within an area of surface crust. The sediment is extremely well sorted with all grains being medium to coarse sand-size. There is a high content (90%) of bioclasts: shallow-water foraminifera (peneroplids), calcareous algae (branched forms), green algae (*Halimeda*, aragonitic, some with evidence of dissolution) and bivalve fragments (Fig. 6b). Volcanic grains are a minor content (10%). Peloids are present in cavities between grains and are probably microbial in origin. The cement is a bladed isopachous calcite, with polygonal junctions between fringes, typical of marine phreatic precipitation (Figs. 6c, d). Acicular aragonite cement occurs within gastropod shells, a syntaxial effect (Fig. 6d).

Sample NA037-026 is a loose sample from an area of rocky outcrops on a quite steep slope (Fig. 7a). It consists of relatively well-sorted granule-small pebble sized volcanic clasts and crystals, many coated with crusts of calcareous red algae (*Amphiroa*, *Lithoporella*), foraminifera (including nubeculariids and acervulinids), serpulids, bryozoans and microbial laminae (Figs. 7b-d). Calcimicrobe filaments are present (like *Girvanellla*), with some being beaded (like *Rothpletzella*, Rob Riding pers. comm.). Pockets of phosphatic peloids are likely also microbial-bacterial. Other bioclasts present include benthic foraminifera (*Amphistegina* and *Archaias*) and echinoids. Evidence of dissolution is present in the form of bivalve and heteropod-gastropod molds (Fig. 7e), some filled with calcite spar. Sponge spicules are also present and show dissolution and replacement by calcite. The patchy cement is mostly a sparry calcite with a drusy fabric. The benthic foraminifera are both from long-ranging

287 genera spanning the Eocene to Holocene and Middle Eocene to Holocene (Boudagher-Fadel,
288 2008) and the random orientation of sections prevents further identification to species level.
289 For both samples 025 and 026 the bioclastic and coated volcanic grain sediment must have
290 formed in much shallower water but then been transported to these deeper locations by either
291 a sediment gravity flow or submarine landslide, where the induration took place. Some
292 deeper-water bioclasts are also present (the heteropods, planktic foraminifera and sponge
293 spicules), probably picked up en-route.
294 In some cases, the cemented slope surfaces are coated with a thin layer of black Mn-Fe
295 oxide-hydroxide, which also occurs on submarine outcrops of volcanic rock. This distinctive
296 surface usually has a very irregular topography of 1-2 cm which likely reflects the effects of
297 boring organisms and local dissolution. Such Fe-Mn oxide coatings are typical of deeper-
298 water lithified surfaces and rock outcrops in areas of sediment starvation and/or where there
299 are quite strong currents sweeping the seafloor. Phosphate (honey-brown colour in thin-
300 section) may also be present, and commonly planktic foraminifera are trapped within the
301 coating. The origin of these Mn-Fe surfaces has been much debated but a bacterial origin is
302 suspected in many cases (Konhauser, 1998). Indeed, tufts of *Frutexites* bacteria have been
303 observed in thin-section of one such coating.
304
305 *4.1.2 Montserrat Submarine Debris Avalanche Deposits*
306 Submarine debris avalanche deposits are a prominent feature of the seafloor around
307 Montserrat (Le Friant et al., 2004; Cassidy et al., 2013; Watt et al., 2015). Off the east coast
308 the youngest debris avalanche, deposit 1, is attributed to the formation of English's Crater by
309 sector collapse at about 4 kyr BP. Three samples of limestone were collected from deposit 1
310 (Fig. 2). Sample NA037-005 (depth 942 m and 12 km offshore) consists of a grey-green
311 micritic pelagic limestone with numerous planktic foraminifera (*Globorotalia*, *Orbicula*),

pteropods, thin-shelled planktic gastropods (heteropods), minor fragments of shallow-water bioclasts (bivalve, foraminifera, echinoid), and silt-sized volcanic crystals. There are some mm-size burrow structures. Samples NA037-002 (975 m depth and 12 km offshore) and NA037-012 (840 m depth and 6 km offshore) are of a similar shallow-water microfacies. Sample NA037-002 is a highly indurated carbonate with coralline algal fragments and small volcanic lithics. Large (cm-size) rhodoliths (nodules of calcareous red algae) occur in a matrix of micrite with many bioclasts, including bivalves, gastropods and benthic foraminifera (*Amphistegina, Archaias* and peneroplids). Patches of drusy calcite spar occur in cavities and occupy moulds of bivalves. Sponge borings occur in the rhodoliths, some filled with microbial peloids. Sample NA037-012 is also coralgal limestone with rhodoliths and a variety of bioclasts including peneroplid foraminifera and bivalves, some showing effects of dissolution and replacement of aragonite by calcite. Encrusting forams and peyssonneliaceae algae are present. Volcanic material is subordinate. Samples 002 and 012 are both shallow-to-moderate (<50 m) depth limestones with typical lagoonal forams. The diagenetic features are consistent with meteoric / freshwater alteration (Tucker and Wright, 1990), although meteoric-type cements can form in deeper water (Schlager and James, 1978; Melim et al., 1995, 2002). Overall, these samples represent limestones from the shallow shelf dislodged and incorporated into the debris avalanche. Sample 002 contains a single probable miogypsinid fragment, which would give a Miocene age; the fragmentary nature of the bioclast however means that reworking is a possibility, although this does agree with the Sr data. However, other genera present again have long ranges from Eocene to Holocene.

4.1.3 Roche's Bluff volcaniclastics, Montserrat

Limestones within a package of submarine volcaniclastics at Roche's Bluff in the SE corner of Montserrat are much fractured and deformed, but fabrics are quite well preserved in thin-section, with some patchy recrystallisation. MacGregor (1938) identified corals, echinoid

spines, serpulids, bivalves and ostracods in the limestones. In our samples the rock is a coralgal limestone with fragments of volcanic rock, many coated with coralline algae and encrusting foraminifera (including nubeculariids). Gastropods and bivalves are present (aragonite shells replaced by calcite), and benthic foraminifera: miliolids, *Amphistegina*, poorly preserved *Archaias*-type forms, miogypsinids, rare planktic foraminifera and agglutinating textularid foraminifera. There are two generations of calcite cement: fibrous fringes and drusy spar, and minor aragonite cement has been replaced by calcite. This limestone was deposited in a shallow-moderate depth, relatively high-energy location. It was subjected to marine cementation and also meteoric dissolution-cementation. The presence of multiple sub-axial sections of *Miogypsina* indicates an early Miocene age in the Americas (BouDagher-Fadel, 2008); the specimens do appear to be complete.

4.1.4 Montserrat Geothermal Wells

Exploration for geothermal energy on Montserrat included three drill-sites. Continuous core was collected in Well Mon3 at depths of 1.5, 1.7 and 2.0 km and rock cuttings were recovered at all levels. Of most relevance here are two horizons of limestone at 2014-2016 m and 930-1020 m depth, within a succession dominated by volcanic, volcaniclastic and intrusive rocks. The limestones at 2014-2016 m, showing evidence of recrystallisation, are mostly fossiliferous wackestone to pack-grainstone from shallow to moderate depths, normal open-marine water. From the foraminifera, a late Miocene age has been assigned (Marcelle BouDagher-Fadel, personal communication). Limestones from depths 1020 to 950 m are also highly fossiliferous and indicate an upward trend from shallower to deeper water. Sample 930 m contains abundant planktic foraminifera, including likely *Orbulina universa,* a single potential *Globergerinoides sacculifer* and potential *Globorotalia* with *Trilobatus trilobus* indicating a likely age in the last 5 Ma.

362

363 *4.1.5 Kick'em Jenny, Southern Lesser Antilles*

364 Two samples are highlighted from the area of Kick'em Jenny submarine volcano in the
365 southern Lesser Antilles (Fig. 2). The first, NA039-071, is a partially indurated carbonate
366 found in proximity to a cold-seep area associated with the distal end of a large debris
367 avalanche on the western slope of KeJ at a depth of 1956 m (Figs. 2, 8a). The seeps host a
368 chemosynthetic-based ecosystem with bivalves, tubeworms, gastropods, crabs and
369 holothurians (Carey et al., 2014a, b, c). The hand-sample contains large burrows, up to 20
370 mm in diameter, some of which are open whereas others contain intraclasts and pellets, up to
371 7 mm in diameter (Fig. 8b, c). In thin-section the sediment consists of grey-green pelagic
372 lime mud and silt with many tiny microfossils including planktic forams (100-500 microns
373 across) and fine skeletal fragments (<200 microns). However, conspicuous are relatively
374 large ostracods, up to 3 mm across (Figs. 8c, d). Some of these ostracods with a mud-fill
375 appear to be part of the large pellets within burrows. Isopachous fibrous-bladed calcite
376 cement occurs locally around the pellets (Fig. 8d). Within one ostracod an acicular cement is
377 present, appearing more like aragonite. Of note, as reported later, this sample has an
378 extremely low $\delta^{13}C$ of -42‰.
379 The second sample, NA039-035, is from the upper slopes of the Kick'em Jack submarine
380 volcano at 172 m depth (Fig. 2) and consists of a mixture of volcanic grains, bioclastic
381 material and lime mud (Fig. 9a). Mafic crystals commonly have a reaction rim. The matrix
382 consists of silt-grade volcanic particles and lime mud which appears to have infiltrated
383 cavities between grains. This mud is vaguely peloidal, but locally it grades into a clear
384 micropeloidal texture. There are pockets of micropeloids, with no matrix between, occurring
385 within cavities which are lined by an initial, very thin isopachous honey-brown amorphous
386 material (Fig. 9b). These micropeloids, 10-30 μm in diameter, appear to have formed within

387 the cavities rather than being washed in, suggesting an in-situ microbial origin. There are also
388 larger peloidal structures (30-60 μm), some coalesced, composed of phosphate. In the
389 patches of lime mud, there are planktic forams, fine bioclastic debris and sponge spicules,
390 replaced by calcite; spicules also occur within empty cavities, which may well have been
391 sponge borings.
392
393 *4.1.6 Kolumbo Seamount Chain, Mediterranean*
394 The numerous seamounts extending northeast from the Santorini caldera show little
395 evidence of recent volcanic activity, with the exception of Kolumbo, which is mostly
396 sediment covered with local outcrops of volcanic rock (Nomikou et al., 2012). Many of the
397 slopes of the seamounts consist of brown, carbonate crusts that are commonly fractured into
398 slab-like pieces. The crusts are typically tens of centimetres to a few metres in thickness with
399 a thin draping of unconsolidated hemipelagic sediment. The sampling locations of three
400 representative samples of carbonate crust from this area are shown in Fig. 2. Samples
401 NA007-001 and NA007-045 are from a small dome complex on the northeast margin of the
402 Kolumbo submarine volcano in water depths of 200 and 128 metres respectively (Fig. 2).
403 Sample NA007-022 was collected from a depth of 194 m on a separate small seamount about
404 7 km northeast of Kolumbo.
405 Sample NA007-001 is a pelagic limestone with many microfossils, planktic forams, thin-
406 shelled bivalves as well as fragments of sponge spicules. The sample itself shows the effects
407 of boring sponges (Fig. 10a). Indeed, an earlier phase of boring has cavities filled with a more
408 brownish lime mud compared to the host lime mudstone that has a more grey colour. Later
409 sponge borings are open and there are modern encrusting serpulids and other organisms
410 present too. Sample NA007-022 (Fig. 10b) has granule to pebble-sized volcanic clasts coated
411 by calcareous red algae, with lime mud containing microfossils between. The sample has also

been bored by sponges and cavities are in places lined by a bladed calcite fringe before a later phase of more microfossiliferous lime mud filling cavities (Figs. 10c, d).

Sample NA007-045 is from slightly deeper water (128 m), on the side of a very small volcanic dome (Figs. 2, 11a). This is a crustose limestone composed of an open framework of foliaceous coralline algae, encrusted with bryozoans and serpulids, with fine-medium sand and volcanic-bioclastic material occurring within the framework cavities (Figs. 11b-d). Fibrous calcite cements occur here as crusts and fans.

These samples from the Hellenic Arc in the Mediterranean are similar to the crusts from the Caribbean: a variable mixture of volcanic and bioclastic material, the biota depending on water depth and degree of downslope reworking of skeletal grains; early cementation commonly by fibrous calcite and micritic calcite; several phases of sponge boring with lime mud, usually pelagic, filling cavities and latest borings still empty, and crusts in deeper water showing thin Fe-Mn coatings.

4.2 Isotope data

Oxygen, carbon and strontium isotopic compositions of limestone samples are presented in Tables 2 and 3. Apparent and approximate ages of carbonate samples can be estimated based on strontium isotopic ratios in comparison with the global seawater strontium isotope curve and data from Neogene carbonates (e.g. Farrell et al., 1995; Howarth and McArthur, 1997 – LOWESS Database 2013; McArthur et al., 2006; McArthur et al., 2012). This approach assumes that the carbonate minerals have been precipitated from seawater and that they have not subsequently been perturbed. However, some of the limestones, notably those from the geothermal well, have ages that are apparently much older than those indicated by foraminifera, suggesting that their initial Sr isotopic compositions have been altered; this is

436 interpreted to have been through contact with geothermal fluids as discussed in more detail
437 below.
438 Figure 12 shows a plot of the $\delta^{13}C$ and $\delta^{18}O$ isotope data. Samples of slope crusts NA037-033
439 and NA037-029 from nearshore SW Montserrat have young Sr isotope ages of less than 200
440 kyr and very similar $\delta^{13}C$ and $\delta^{18}O$, averaging +3.6 ‰ and 2.25 ‰ respectively. The $\delta^{13}C$ are
441 within the usual range of marine sediments (Tucker and Wright, 1990), whereas the $\delta^{18}O$ is a
442 little more positive than might be expected for a tropical carbonate (e.g. Swart, 2015),
443 possibly since the sediment was cemented in water > hundred metres deep, which would have
444 been quite cool (~13-20 ^{o}C), compared with a near-surface water temperature of 28-30 ^{o}C
445 (Kameo et al., 2004). Sample NA037-025 from offshore SW Montserrat also has a young Sr
446 isotope age (a few 100 kyr) and similar marine values for both $\delta^{13}C$ (+3.2‰) and $\delta^{18}O$
447 (+2.5‰). In contrast, sample NA037-026 has a much older apparent Sr isotope age (17-20
448 Ma) and low negative stable isotope values of both $\delta^{13}C$ of -2.3‰ and $\delta^{18}O$ -3.8‰,
449 suggesting alteration.
450 The three limestone clasts collected from Montserrat debris-avalanche Deposit 1 on the
451 eastern side of the island have diverse isotope geochemistry. The pelagic limestone (sample
452 NA037-005) has a very young Sr isotope age (<100 kyr) and typical marine values for $\delta^{13}C$
453 and $\delta^{18}O$. The two coralgal limestone clasts (NA037-002 and NA037-012) have yielded
454 much older Sr age dates, especially sample NA037-002, of 23-25 Ma (early Miocene),
455 whereas sample NA037-012 is 975 kyr to 1.5 Ma (Table 3). For the C and O isotopes,
456 sample NA037-012 has low positive values (Fig. 12), both likely marine. Sample NA037-
457 002, on the other hand, has a more typical marine $\delta^{13}C$ signature (+2‰) but $\delta^{18}O$ varies, with
458 4 negative values (-2.5 to -3.6‰) and one of +2‰. The negative $\delta^{18}O$ values are consistent
459 with some alteration, likely meteoric, reflecting the low negative isotopic composition of
460 freshwater (mean rainfall is ~-4‰ $\delta^{18}O$ VSMOW for Barbados for example). The $\delta^{13}C$ values

461 indicate recycling of the original marine carbonate, rather than any effect of soil CO_2 gas
462 which would be enriched in (biogenic) ^{12}C (Tucker and Wright, 1990).
463 Roche's Bluff limestone samples also yield apparent old Sr isotope ages: 16.5 and 17.1 Ma
464 (early Miocene), which are inconsistent with other age data, such as the $^{40}Ar/^{39}Ar$ age of
465 1.021 ±0.020 Ma from a volcanic clast in the Roche's Bluff Submarine Volcaniclastic unit
466 and the <1.8 Ma age suggested by the identification of the foraminifera species *Globorotalia*
467 *truncatulinoides* (Harford et al., 2002). However, the presence of several *Miogypsina* in the
468 thin-sections would support a Miocene age, although other larger foraminifera present only
469 indicate Eocene to Recent. The $\delta^{13}C$ values are normal marine (average +2.1‰). However,
470 $\delta^{18}O$ is very negative at -7.7‰; this is too low for rainfall of this latitude for it to be simply a
471 meteoric / freshwater effect. An alternative explanation is that the low negative $\delta^{18}O$ of the
472 Roche's Bluff limestone was generated by recrystallisation (recorded in thin-section) under
473 moderate-high temperatures through interaction with hydrothermal fluids. This would also
474 account for the apparent old Sr ages, if the miogypsinids are reworked. Such hydrothermal
475 fluids, with a low Sr isotope value derived from passage through volcanics, may have been
476 introduced through the fault system adjacent to the Roche's Bluff outcrops.
477 For limestones in the geothermal well Mon3 the apparent Sr isotope ages are all much older
478 than the ages based on fossils and unpublished $^{40}Ar/^{39}Ar$ data. The core samples of upper
479 Miocene (~5-7 Ma) limestone at 2 km depth give much older apparent Sr ages in the range
480 16.7-19.7 Ma. Cuttings samples from 930 m and from 1198 m depth are also apparently old:
481 4 analyses give an age of around 15 Ma, although one analysis yielded an age of 0.55 Ma; the
482 planktic foraminifera do suggest a young age. Unpublished $^{40}Ar/^{39}Ar$ ages of andesites at
483 depths of 1.5 and 1.7 km depth are approximately 1 Ma old. The C and O isotope data from
484 two (whole-rock) limestone core samples both have negative $\delta^{13}C$ and $\delta^{18}O$. For one sample
485 (2015 m depth) $\delta^{13}C$ values (4 analyses) are low (average -0.75‰), with very negative $\delta^{18}O$

(average -10.3‰). For sample depth 2016 m, $\delta^{13}C$ values (2 analyses) are more negative (average –3.2‰) and $\delta^{18}O$ is on average -9.4‰. One analysis from a thick-shelled bivalve in that 2016 m sample has $\delta^{13}C$ of +1.9 and $\delta^{18}O$ of –11.2‰. The negative $\delta^{13}C$ values are likely the result of decomposition of organic carbon within the sediments, producing isotopically light CO_2. For cuttings samples (930 m to 1198 m), $\delta^{13}C$ and $\delta^{18}O$ are around +2‰ for $\delta^{13}C$, a typical marine carbonate value, but $\delta^{18}O$ is -8‰, again suggesting significant alteration related to burial diagenesis / interactions with hydrothermal fluids although this had no effect on the $\delta^{13}C$, possibly related to issues around supply or availability of C in the fluid.

These Sr and stable isotope analyses from the Mon3 well all indicate post-depositional alteration of the original seawater-marine values, most likely by interaction with hydrothermal-volcanic fluids. The apparent old ages are the result of introducing a component of volcanic non-radiogenic Sr into the carbonates. $^{87}Sr/^{86}Sr$ of Montserrat volcanic rocks are in the narrow range 0.7035 to 0.7038 (Cassidy et al., 2012). The Sr in the geothermal fluids will be largely derived from the volcanic rocks and this will exchange with or add to the limestones' initial Sr. Likewise, the strongly negative $\delta^{18}O$ reflects geothermal fluid interactions. We surmise that the anomalously old Sr ages and negative $\delta^{18}O$ in samples from the Deposit 5 debris avalanche (NA037-026), the Deposit 1 debris avalanche (NA037-002) and the Roche's Bluff limestone, are also the consequence of hydrothermal alteration of shelf limestones.

5. Discussion

We propose a conceptual model for the development of the limestone crusts based on established groundwater models for coastal regions and volcanic islands (Cooper, 1959; Join et al., 2005), perturbed by the development of a hydrothermal system (Fig. 13). Montserrat broadly conforms to this conceptual model (Hemmings et al., 2015) of a freshwater lens

above sea level and saline (seawater) intrusion beneath with a transitional mixing-zone occurring close to the coast. Freshwater outflows at the coast are balanced by recharge and seawater inflow below sea level. The hydrogeology on Montserrat is significantly perturbed due to the development of a geothermal field along the Belham Valley fault system (Ryan et al., 2013) and the presence of an active hydrothermal system associated with the SHV edifice. Several scattered fumaroles and hot springs have been present historically (Chiodini et al., 1996), although these systems were disrupted by the 1995-2010 eruption. The Belham Valley geothermal field contains brines with the approximate salinity of seawater, but with a geochemistry suggestive of interaction with volcanic rocks. Temperatures up to 230 ^{o}C are recorded in the geothermal wells.

We envisage that the carbonate crusts largely developed as a result of carbonate-saturated seawater fluxing through the submarine flanks of the island, precipitating carbonate cement in the pores of the sediments. The $\delta^{13}C$ and $\delta^{18}O$ values of many of the crust samples indicate a seawater origin. In the classic coastal hydrological model (Fig. 13) the main driver is the density difference between seawater and fresh groundwater in the volcanic edifice. The subaerial flanks of the volcano are composed of high permeability and high porosity volcaniclastic deposits which create the main aquifer (Hemmings et al., 2015). Two factors can enhance the submarine inflow of seawater into the volcanic edifice. Upwelling of hot geothermal and hydrothermal magmatic fluids within the volcanic island is expected to cause inward flow of groundwater and underlying brines, strengthening the inflow of seawater. The process of Kohout convection, driven by geothermal heat, has been invoked as a mechanism for drawing seawater into carbonate shelves and isolated platforms, and precipitating dolomite (Whitaker and Smart, 1990). In addition, inflow will be increased during periods of sea-level rise due to the increased hydraulic head in the ocean (Tucker, 1993; Kim et al., 2010); there have been changes in sea level on the scale of 100 m many times over the last

few million years as a result of the waxing and waning of Quaternary ice sheets. The inflow, however, may decrease as the carbonate crust forms, with consequent reduction of porosity and permeability, so that the formation of the crust may then promote sealing of the island interior from seawater intrusion.

The formation of hardgrounds in the deeper-water slope environment from influxing seawater is controlled by several factors, but notably carbonate saturation, the movement of fluid through sediment (the 'hydrodynamic level' of Christ et al., 2015) and microbial activities, as well as temperature and a sediment's poroperm. At the depths of less than 1000 m where the cemented crusts occur seawater will be saturated with respect to $CaCO_3$, even though seafloor temperatures will be down to 5^{o}C (Kameo et al., 2004). The circulation of fluid through sediment is essential to drive cement precipitation and here waves and tides, internal waves and ocean currents impinging on a slope may all be involved (van der Kooij et al., 2010). In addition, circulation driven by geothermal heat within the seamount, as discussed above, is likely to contribute to drawing in water from the adjacent sea (Jones et al., 2000). With regard to microbial influences, some bacteria promote carbonate precipitation, notably the cyanobacteria and sulphate reducers, by raising alkalinity, whereas others, such as aerobic heterotrophs and fermenters, may lead to local carbonate dissolution through reducing pH in their metabolic processes (Dupraz et al., 2009).

Reviewing the diagenesis observed within the crusts, the most common cement is calcite, in many cases a bladed-fibrous type, particularly as an isopachous rim around grains in the more porous well-sorted, sand-grade deposits. Other crusts have a drusy sparry calcite cement within cavities. Acicular aragonite crystals mostly occur as syntaxial precipitates on originally aragonitic skeletal fragments, especially gastropods. Evidence of aragonite dissolution and replacement is provided by molds of bivalves, some filled with calcite; sponge spicules (originally opaline silica) have also been replaced by calcite, with crystals

561 extending out into cavities. Several phases of boring by sponges are evident as well as phases
562 of internal sedimentation. Micritic peloids are a feature of many crusts, occurring within
563 intraskeletal cavities, borings and between grains, and in some cases there is gradation into
564 micritic sediment. Microbial filaments are also present but they can be difficult to distinguish
565 from nubeculariid foraminifera or thin poorly-preserved coralline algal crusts. Dissolution of
566 the surface of the hardgrounds is evident from their irregular microtopography and a mm-
567 thick layer of Mn-Fe oxide coating is a common feature. All in all, the paragenesis of these
568 crusts is commonly a complex series of cementation-alteration-boring-dissolution events.
569 All the features of the crusts are consistent with the volcaniclastic-carbonate sediment being
570 cemented and altered on the seafloor in the marine environment. They are similar to crusts
571 reported by Thompson et al. (1968), Schroeder et al. (2002), McKenzie and Bernoulli (1982)
572 and Buchs et al. (2018). The bioclastic material in the slope limestones described here is
573 dominated by calcareous algae, especially in the form of rhodoliths, encrusting volcanic
574 grains, and foraminifera, both benthic and planktic, the former commonly derived from
575 shallower water. Rhodoliths are a common feature of limestones associated with
576 volcaniclastic and volcanic rocks, especially in the moderate to high-energy settings of open-
577 ocean seamounts and islands (e.g. Madeira and the Azores; Baarli et al., 2014; Rebelo et al.,
578 2016). Calcite spar as a cement is usually regarded as a near-surface meteoric or burial
579 precipitate, but there are records of it occurring on the seafloor in deeper water (Melim et al.,
580 1995, 2002). Slower rates of precipitation in cooler water are the likely explanation. Cooler
581 water and its circulation through the surficial crusts are likely to account for aragonite
582 dissolution and replacement, again a feature commonly ascribed to freshwater diagenesis
583 (Tucker and Wright, 1990). Petrographic evidence for microbial activity is being recognized
584 more frequently as the significance of microbes in mineral precipitation is becoming
585 appreciated (e.g., Perri et al., 2018). Here in these crusts, communities of bacteria living

586 within the sediment are implicated by the occurrence of the peloidal micrite and it may well
587 be that microbial processes have contributed to the lithification of the slope sediment.
588 Most of the limestones in the geothermal wells, two clasts of shallow-water limestone taken
589 from debris-avalanche deposits, and the Roche's Bluff limestone, all show isotopic evidence
590 for hydrothermal alteration with very negative $\delta^{18}O$ and $^{87}Sr/^{86}Sr$ compositions that indicate
591 ages from the seawater calibration curve that appear to be too old. We infer that these
592 limestones have been affected by the volcanogenic hydrothermal systems that developed
593 within the island interior. The observed alteration testifies to largescale hydrothermal
594 convection throughout the island's history.
595 The formation of these crusts is inferred to be in the mature stage of volcanic edifice growth.
596 Each of the volcanic centres initially formed on the seafloor at water depths of 800 to 1000 m
597 and grew to a height of the order of 1000 m above sea level, as is the case for the still active
598 Soufrière Hills Volcano. For a constant rate of volcanism the lateral speed of advance of the
599 volcanoes' flanks will slow; for example if the edifice is treated as a cone with a constant
600 height to width ratio then the lateral speed will decrease in proportion to $t^{-2/3}$.
601 There is geomorphological evidence for the stabilisation of the submarine flanks of
602 Montserrat and their preservation for long periods of time. Le Friant et al. (2004) compared
603 several topographic profiles around Montserrat from the shallow shelves to deep water. The
604 overall width of the shallow part of the island stays approximately the same from north to
605 south (Fig. 1) whereas the shallow shelf decreases in width. The profiles from the shelf edge
606 to deep water are very similar. These observations suggest that the submarine parts of the
607 islands stabilize after the volcano becomes extinct, which can be explained by the formation
608 of the limestone crust which prevents inward erosion by mass wasting. The widening of the
609 shallow shelf from south to north was interpreted by Le Friant et al. (2004) as the
610 consequence of lateral erosion of the island during glacial high stands due to wave and storm

611 erosion. However, there is new evidence for regional subsidence (Carey et al., 2019) and so
612 the widening of the platform to the north could also reflect subsidence of the three volcanic
613 centres on Montserrat, which become older to the north. In either case the platform outer
614 edge will approximately reflect the width of the final edifice at the cessation of volcanic
615 activity.
616 On the western side of Montserrat, there is further evidence for stabilisation of the submarine
617 flanks from the marked embayments and southward narrowing of the shelf. This zone is the
618 location of where active faults of the Havers-Montserrat fault system intersect the island. We
619 suggest that faulting in this zone has disrupted the limestone crust and promoted mass-
620 wasting of the submarine flanks.
621 Furthermore, episodes of sector collapse can play an important role in that they would
622 channelize lahars and pyroclastic flows down preferential pathways, as exemplified by the
623 Tar River Valley on the eastern flanks of Montserrat. As a consequence, large sections of
624 submarine coast will be abandoned with lateral growth reducing or ceasing, providing
625 conditions for thick limestone crust to form.

626 **6. Conclusions**

627 Remotely-operated vehicle (ROV) explorations of shallow to moderately deep seamounts in
628 many subduction zone environments, such as the Lesser Antilles (West Indies) and Hellenic
629 Arc (Greece), reveal the existence of extensive carbonate crusts on their submarine flanks.
630 These crusts are composed of mixtures of volcaniclastic debris and bioclastic material, in
631 most cases cemented by calcite, in the form of isopachous coatings around grains or pore-
632 filling spar. $^{87/86}Sr$ isotope data give an indication of age but also demonstrate that some
633 samples are altered by hydrothermal-volcanic processes, as shown by ages much older than
634 expected. Such alteration is also supported by $\delta^{13}C$ and $\delta^{18}O$ isotope data, although most
635 samples possess typical marine values, with the $\delta^{18}O$ commonly a little more positive, likely

reflecting cooler water at the depth of carbonate lithification. The occurrence of such crusts on the slopes of seamounts and volcanic islands is significant from two perspectives. First, they represent a new location of limestone deposition in the World's oceans. Second, the hardgrounds act to protect the submarine flanks of volcanic islands and seamounts from erosion and collapse and they may inhibit submarine intrusion of seawater into the interior of such volcanic edifices. In addition, they also form important hard substrates for the development of benthic biological communities.

Acknowledgements

Leverhulme Trust Emeritus Fellowship to RSJS. We are grateful to Marcelle BouDagher-Fadel for the identification of foraminifera in the well Mon3 core samples, to Paul Pearson for advice on planktic foraminifera, to Juan Carlos Braga for comments on coralline algae and Rob Riding for thoughts on calcimicrobes. NERC are thanked for funds to allow coring of the Montserrat geothermal drill holes and the BGS for archiving of and access to the cores. Operations of the E/V Nautilus were supported through grants from NOAA Office of Ocean Exploration. We thank Nicole Raineault for her assistance in producing bathymetric maps around the island of Montserrat.

References

Aghib, F.S., Weissert, H., Bernoulli, D., 1991. Hardground formation in the Bannock Basin, Eastern Mediterranean. Mar. Geol. 100, 103–113.

Allouc, J., 1990. Quaternary crusts on slopes of the Mediterranean Sea: a tentative explanation for their genesis. Mar. Geol. 94, 205–238.

Avanzinelli R., Boari E., Conticelli S., Francalanci L., Guarnieri L., Perini G., Petrone, Chiara M., Tommasini S., Ulivi M., 2005. High Precision Sr, Nd and Pb Isotopic Analyses Using the New Generation Thermal Ionisation Mass Spectometer ThermoFinnigan Triton-Ti. Periodico Di Mineralogia 74, 147–66.

Baarli, B.G., Cachão, M., da Silva C.M., Johnson, M.E., Mayoral, E.J., Santos, A., 2014. A Middle Miocene carbonate embankment on an active volcanic slope: ilhéu de Baixo, Madeira Archipelago, Eastern Atlantic. Geol. J. 49, 90–106.

Birck, J.L., 1986. Precision K-Rb-Sr isotopic analysis: application to Rb-Sr chronology. Chem. Geol. 56, 73-83.

Boudagher-Fadel, M. K., 2008. Evolution and geological significance of larger benthic foraminifera. Amsterdam: Elsevier, Developments in Palaeontology and Stratigraphy, 21, 544 p.

Buchs, D.M., Williams, R., Sano, S.I., Wright, V.P., 2018. Non-Hawaiian lithostratigraphy of Louisville seamounts and the formation of high-latitude oceanic islands and guyots. Journal of Volcanology and Geothermal Research 356, 1-23.

Carey, S., Bell, K.L.C., Nomikou, P., Vougioukalakis, G., Roman, C.N., Cantner, K., Bejelou, K., Bourbouli, M., Martin, J.F., 2011. Exploration of the Kolumbo Volcanic Ri Zone. In K.L.C. Bell and S.A. Fuller (eds.), New Frontiers in Ocean Exploration: E/V Nautilus 2010 Field Season. Oceanography 24, supplement, pp. 24-25. https://doi. 10.5670/oceanog.24.1.supplement

686 Carey, S., Bell, K.L.C., Sparks, R.S.J., Stinton, A., Ausubel, J., Phillips, B., Raineault, N.,
687 Siu, N., Fandel, C., Graham, O., Ramsingh, H., Blake, R., Auscavitch, S., Demopoulos, A.,
688 Rodrigue, K., 2014a. Impact of volcanic eruptions on the seafloor around Montserrat, West
689 Indies. In: Bell, K.L.C., M.L. Brennan, and N.A. Raineault, eds. 2014. New Frontiers in
690 Ocean Exploration: The E/V Nautilus 2013 Gulf of Mexico and Caribbean Field
691 Season. Oceanography 27(1), supplement, 52 pp,
692 https://doi.org/10.5670/oceanog.2014.supplement.01.
693
694 Carey, S., Bell, K.L., Ballard, R.D., Roman, C., Dondin, F., Miloslavich, P., Gobin, J.,
695 Seibel, B., Smart, C., Fuller, S., Siu, N., 2014b. Fluid/gas venting and biological communities
696 at Kick'em Jenny submarine volcano, Grenada (West Indies). Oceanography 27, 38-41.
697
698 Carey, S., Ballard, R., Bell, K. L. C., Bell, R. J., Connally, P., Dondin, F. et al., 2014c. Cold
699 seeps associated with a submarine debris avalanche deposit at Kick'em Jenny volcano,
700 Grenada (Lesser Antilles). Deep-Sea Research Part I- Oceanographic Research Papers 93,
701 156– 160. https://doi.org/10.1016/j.dsr.2014.08.002
702
703 Carey, S., Bell, K. L.C., Roman, C., Dondin, F., Robertson, R., Gobin, J., Wankel, S.,
704 Michel, A.P.M., Amon, D.J., Marsh, L., Smart, C. Vaughan, I., Ball, B., Rodrigue, K.,
705 Haldeman, M., George, A., Ballard, R., 2015. Exploring Kick'em Jenny submarine volcano
706 and the Barbados Cold Seep Province, Southern Lesser Antilles [in special issue: New
707 Frontiers in Ocean Exploration: The E/V Nautilus 2014 Gulf of Mexico and Caribbean Field
708 Season]. Oceanography 28 (1, Supplement), 38-39.
709

Carey, S., Sparks, R.S.J., Tucker, M.E., Robertson, L., Watt, S.F.L., Gee M., Hastie, A., Li, T., Barfod, D.N., Stinton, A., Raineault, N. and Ballard, R.B.D. 2019. The polygenetic Kahouanne Seamounts in the Northern Lesser Antilles Island Arc: Evidence for large-scale volcanic island subsidence. Marine Geology 419, 10646.

Cassidy, M., Taylor, R.N., Palmer, M.R., Cooper, R.J., Stenlake, C., Trofimovs, J., 2012. Tracking the magmatic evolution of island arc volcanism: Insights from a high-precision Pb isotope record of Montserrat, Lesser Antilles. Geochem. Geophys. Geosyst. 13, Q05003, doi:10.1029/2012GC004064.

Cassidy, M., Trofimovs, J., Palmer, M.R., Talling, P.J., Watt, S.F.L., Moreton, S.G., Taylor, R.N., 2013. Timing and emplacement dynamics of newly recognized mass flow deposits at ~8–12 ka offshore Soufrière Hills volcano, Montserrat: How submarine stratigraphy can complement subaerial eruption histories. Journal of Volcanology and Geothermal Research 253, 1-14.

Chiodini, G., Cioni, R., Frullani, A., Guidi, M., Marini, L., Prati, F., Raco, B., 1996. Fluid geochemistry of Montserrat Island, West Indies. Bull. Volcanol. 58, 380–392.

Christ, N., Immenhauser, A., Wood, R.A., Darwich, K., Niedermaya, A., 2015. Petrography and environmental controls on the formation of Phanerozoic marine carbonate hardgrounds. Earth-Science Reviews 151, 176–226.

Cooper, H.H., 1959. A hypothesis for the dynamic balance of freshwater and saltwater in a coastal aquifer. Journal of Geophysical Research 64, 461-467.

Coussens, M., Cassidy, M., Watt, S. F. L., Jutzeler, M., Talling, P. J., Barfod, D. et al., 2017. Long-term changes in explosive and effusive behaviour at andesitic arc volcanoes: Chronostratigraphy of the Centre Hills Volcano, Montserrat. Journal of Volcanology and Geothermal Research 333–334, 15–35. https://doi.org/10.1016/j.jvolgeores.2017.01.003.

Darwin, C., 1874. The Structure and Distribution of Coral Reefs. Revised edition. London: Smith, Elder & Co. 1874.

Devas, R.P., 1974. History of the Island of Grenada, pp. 1498–1796, Carenage Press, St. George's, Grenada.

Dondin, F., Lebrun, J.F., Kelfoun, K., Fournier, N., Randrianasolo, A., 2012. Sector collapse at Kick'em Jenny submarine volcano (Lesser Antilles): Numerical simulation and landslide behavior. Bull. Volcanol. 74, 595–607.

Dravis, J., 1979. Rapid and widespread generation of Recent oolitic hardgrounds on a high energy Bahamian platform, Eleuthera bank, Bahamas. J. Sediment. Petrol. 49, 195–207.

Dupraz, C.R., P., R., Braissant, O., Decho, A.W., Norman, R.S., Visscher, P.T., 2009. Processes of carbonate precipitation in modern microbial mats. Earth Sci. Rev. 96, 141–162.

Farrell, J.W., Clemens, S.C., Gromet, P.L., 1995. Improved chronostratigraphic reference curve of late Neogene seawater $^{87}Sr/^{86}Sr$. Geology 23, 403–406.

760

761 Feuillet, N., Leclerc, F. Tapponnier,P., François Beauducel, F., Boudon,G., Le Friant, A.
762 Deplus, C., Lebrun, J-F., Nercessian, A., Saurel, J-M., Clément, V., 2010. Active faulting
763 induced by slip partitioning in Montserrat and link with volcanic activity: new insights from
764 the 2009 GWADASEIS marine cruise data. Geophysical Research Letters 37, L00E15,
765 https://dx.doi.org/10.1029/2010GL042556

766

767 Harford, C. L., Pringle, M. S., Sparks, R. S. J., Young, S. R., 2002. The volcanic evolution of
768 Montserrat using $^{40}Ar/^{39}Ar$ geochronology. In T. H. Druitt & B. P. Kokelaar (Eds.), The
769 eruption of the Soufrière Hills Volcano, Montserrat from 1995 to 1999 (Vol. 21, pp. 93–113).
770 London, UK: Geological Society Memoirs.
771 https://doi.org/10.1144/GSL.MEM.2002.021.01.05

772

773 Hatter, S.J., Palmer, M.R., Gernon, T.M., Taylor, R.N., Cole, P.D., Barfod, D.N., Coussens,
774 M., 2018. The evolution of the Silver Hills volcanic center, and revised $^{40}Ar/^{39}Ar$
775 geochronology of Montserrat, Lesser Antilles, with implications for island arc volcanism.
776 Geochemistry, Geophysics, Geosystems 19. https://doi.org/10. 1002/2017GC007053.

777

778 Hemmings, B., Whitaker, F., Gottsmann, J., Hughes, A., 2015. Hydrogeology of Montserrat,
779 review and new insights. Journal of Hydrology: regional studies 3, 1-30.

780

781 Horwitz, E.P., Chiarizia, R., Dietz, M.L., 1992. A novel strontium-selective extraction
782 chromatographic resin. Solvent Extr. Ion Exch. 10, 313–336.

783

784 Howarth, R.J., McArthur, J.M. (1997) Statistics for strontium isotope stratigraphy: A robust
785 LOWESS fit to the marine Sr-isotope curve for 0 to 206 Ma, with look-up table for derivation
786 of numeric age. Journal of Geology 105, 441–456.
787
788 Join, J-L., Folio, J-L., Robineau, B., 2005. Aquifers and groundwater within active shield
789 volcanoes. Evolution of conceptual models in the Piton de la Fournaise volcano. Journal of
790 Volcanology and Geothermal Research 147, 187– 201
791
792 Jones, G., Whitaker, F., Smart, P., Sanford, W. (2000) Numerical modelling of geothermal
793 and reflux circulation in Enewetak Atoll: implications for dolomitization. J. Geochem.
794 Explor. 69-70, 71–75.
795
796 Kameo, K., Shearer, M.C., Droxler, A.W., Mita, I., Watanabe, R., Sato, T., 2004. Glacial–
797 interglacial surface water variations in the Caribbean Sea during the last 300 ky based on
798 calcareous nannofossil analysis. Palaeogeography, Palaeoclimatology, Palaeoecology 212,
799 65– 76.
800
801 Kenedi, C.L, Sparks, R.S.J., Malin, P.E., Voight, B., Dean, S., Minshull, T., Paulatto, M.,
802 Peirce, C., Shalev, E., 2010. Contrasts in morphology and deformation offshore Montserrat:
803 New insights from the SEA-CALIPSO marine cruise data. Geophysical Research Letters 37,
804 L00E25, doi:10.1029/2010GL043925.
805
806 Kim K-Y., Park, E., Han W.S., 2010. Effect of a high permeable layer on hydraulic system in
807 a coastal aquifer. SWIM21 - 21st Salt-Water Intrusion Meeting, Azores Portugal, 359- 362.
808

809 Konhauser, K.O., 1998. Diversity of bacterial iron mineralization. Earth Sci. Rev. 43, 91–
810 121.
811
812 Kokelaar, B.P., 2002. Setting, chronology and consequences of the eruption of Soufrière Hills
813 Volcano, Montserrat (1995-1999). *In* Druitt, T.H. and Kokelaar, B.P., The Eruption of the
814 Soufrière Hills Volcano, Montserrat, From 1995 to 1999, Geological Society, London,
815 Memoirs 21, 1–43. https://doi.org/10.1144/GSL.MEM.2002.021.01.02
816
817 Le Friant, A., Harford, C.L., Deplus, C., Boudon, G., Sparks, R.S.J., Herd, R.A.,
818 Komorowski, J.C., 2004. Geomorphological evolution of Montserrat (West Indies):
819 importance of flank collapse and erosional processes. Journal of the Geological Society of
820 London 161, 147-160.
821
822 Le Friant, A., Deplus, C., Boudon, G., Sparks, R.S.J., Trofimovs, J., Talling. P.J., 2009.
823 Submarine deposition of volcaniclastic material from the 1995-2005 eruptions of Soufrière
824 Hills Volcano, Montserrat. Journal of the Geological Society of London 166, 171-182.
825
826 Lewis, J., Coath, C., Pike, A., 2014. An improved protocol for $^{87}Sr/^{86}Sr$ by laser ablation multi-
827 collector inductively coupled plasma mass spectrometry using oxide reduction and a
828 customised plasma interface. Chemical Geology 390, 173-181.
829
830 Lindsay, J., Shepherd, J.B., Wilson, D., 2005. Volcanic and scientific activity at Kick'em
831 Jenny submarine volcano 2001-2002: Implications for volcanic hazards in the southern
832 Grenadines, Lesser Antilles. Nat. Hazard 34, 1–24.
833

834 Macgregor, A.G., 1938. The Royal Society Expedition to Montserrat, B.W.I. The volcanic
835 history and petrology of Montserrat with observations on Mt Pele, in Martinique.
836 Philosophical Transactions of the Royal Society of London B229, 1-90.
837
838 Malone, M.J., Slowey, N.C., Henderson, G.M., 2001. Early diagenesis of shallow-water
839 periplatform carbonate sediments, leeward margin, Great Bahama Bank (Ocean Drilling
840 Program Leg 166). GSA Bull. 113, 881–894.
841
842 McArthur, J.M., Howarth, R., Shields, G., 2012. Strontium isotope stratigraphy. In: the
843 Geologic Time-Scale. Elsevier pp. 127–144.
844
845 McArthur, J.M., Rio, D., Massari, F., Castradori, D., Bailey, T.R., Thirlwall, M., Houghton,
846 S., 2006. A revised Pliocene record for marine $^{87}Sr/^{86}Sr$ used to date an interglacial event
847 recorded in the Cockburn Island Formation, Antarctic Peninsula. Palaeogeography,
848 Palaeoclimatology, Palaeoecology 242, 126–136.
849
850 McKenzie, J.A., Bernoulli, D.,1982. Geochemical variations in Quaternary hardgrounds from
851 the Hellenic Trench region and possible relationship to their tectonic setting. Tectonophysics.
852 86: 149-157. https//doi.10.1016/0040-1951(82)90065-8
853
854 Melim, L.A., Swart, P.K., Maliva, R.G., 1995. Meteoric-like fabrics forming in marine
855 waters: Implications for the use of petrography to identify diagenetic environments. Geology
856 23, 755-758.
857

Melim, L.A., Westphal, H., Swart, P.K., Eberli, G.P., Munnecke, A., 2002. Questioning carbonate diagenetic paradigms: evidence from the Neogene of the Bahamas. Marine Geology 185, 27-53.

Milliman, J.D., 1974. Marine Carbonates. Springer-Verlag, Berlin.

Murray, J., Renard, A.F., 1891. Report on deep-sea deposits. Report on the Scientific Results of the Voyage of H.M.S. Challenger During the Years 1873–76. Neill and Co., Edinburgh.

Nier, A.O., 1938. The isotopic constitution of strontium, barium, bismuth, thallium and mercury. Physical Review 54, 275–78.

Noé, S., Titschack, J., Freiwald, A., Dullo, W.-C., 2006. From sediment to rock: diagenetic processes of hardground formation in deep-water carbonate mounds of the NE Atlantic. Facies 52, 183–208.

Nomikou, P., Carey, S., Papanikolaou, D., Croff Bell, K., Sakellariou, D., Alexandri, M., Greece. Global and Planetary Change, 90-901, 135-151.

Perri, E., Tucker, M.E., Słowakiewicz, M., Whitaker, F., Bowen, L., Perrotta, I., 2018. Carbonate and silicate biomineralization in a hypersaline microbial mat (Mesaieed Sabkha, Qatar): roles of bacteria, EPS and viruses. Sedimentology, 65, 1213-1245.

Poux, B., Brophy, P., 2012. Geothermal exploration on the island of Montserrat, Caribbean. GRC Transactions, 36, 737–744.

Rea, W.J., 1974. The volcanic geology and petrology of Montserrat, West Indies. Journal of the Geological Society, London 130, 341–366.

Rebelo, A.C., Rasser, M., Kroh, A., Johnson, M.E., Melo, C., Ramalho, R.S., Uchman, A., Zanon, V., Silva. L., Neto, A., Berning, B., Cachão, M., Ávila, S., 2015. Rocking around a volcanic island shelf: Neogene rhodolith beds from Malbusca, Santa Maria Island (Azores, NE Atlantic). Facies 62, 22-31.

Russell W., Papanastassiou D., Tombrello T. 1978. Ca isotope fractionation on the Earth and other solar system materials. Geochimica et Cosmochimica Acta 42, 1075–90.

Ryan, G.A., Peacock, J.R., Shalev, E., Rugis, J., 2013. Montserrat geothermal system: A 3D conceptual model. Geophysical Research Letters 40, 1-6.

Schlager, W., James, N.P., 1978. Low-magnesian calcite limestones forming on the deep seafloor, Tongue of the Ocean, Bahamas. Sedimentology 25, 675–702.

Schroeder, T., John, B., Frost, B.R., 2002. Geologic implications of seawater circulation through peridotite exposed at slow-spreading mid-ocean ridges. Geology 30, 367–370.

Shepherd, J. B., Robson, G.R., 1967. The source of the T-phase recorded in the Eastern Caribbean on October 24, 1965. Bull. Seismol. Soc. Am. 57, 227–234.

907 Shinn, E.A., 1969. Submarine lithification of Holocene carbonate sediments in the Persian
908 Gulf. Sedimentology 12, 109–144.
909
910 Sigurdsson, H., Shepherd, J.B., 1974. Amphibole-bearing basalts from the submarine volcano
911 Kick'em Jenny in the Lesser Antilles arc. Bull. Volcanol. 28, 891–910.
912
913 Sigurdsson, H., Carey, S., Wilson, D., 2006. Debris Avalanche Formation at Kick'em Jenny
914 Submarine Volcano, 66 pp., World Scientific, Hackensack, N. J.
915
916 Steiger, R., Jäger E., 1977. Subcommission on Geochronology: Convention on the use of
917 decay constants in geo-and cosmochronology. Earth and Planetary Science Letters 36, 359–
918 62.
919
920 Stoddart, D.R., 1976. Darwin, Lyell, and the geological significance of coral reefs. British
921 Journal for the History of Science 9, 199–218.
922
923 Swart, P., 2015. The geochemistry of carbonate diagenesis: The past, present and future.
924 Sedimentology 62, 1233–1304.
925
926 Thirlwall, M.F., 1991, Long-term reproducibility of multicollector Sr and Nd isotope ratio
927 analysis. Chemical Geology 94, 85-104.
928
929 Thompson, G., Bowen, V.T., Melson, W.G., Cifelli, R., 1968. Lithified carbonates from the
930 deep-sea of equatorial Atlantic. J. Sediment. Petrol. 38, 1305–1312.
931

Trofimovs, J., Foster, C., Sparks, R.S.J., Loughlin, S., Le Friant, A., Deplus, C., Porritt, L., Christopher, T., Luckett, R., Talling, P.J., Palmer, M.R., Le Bas, T., 2012. Submarine pyroclastic deposits formed during the 1 20th May 2006 dome collapse of the Soufrière Hills volcano. Montserrat. Bulletin of Volcanology 74, 395-401.

Tucker, M.E., 1993. Carbonate diagenesis and sequence stratigraphy. In: Sedimentology Review (Ed. V.P. Wright) 1, 51-72.

Tucker, M.E., Wright, V.P., 1990. Carbonate Sedimentology. Blackwell Science. Oxford.

van der Kooij, B., Immenhauser, A., Steuber, T., Bahamonde, J.R., Merino Tomé, O., 2010. Precipitation mechanisms of volumetrically important early marine carbonate cement volumes in deep-slope settings. Sedimentology 57, 1491–1525.

van der Land, C., Mienis, F., De Haas, H., Frank, N., Swennen, R., Van Weering, T.C.E., 2010. Diagenetic processes in carbonate mound sediments at the south-west Rockall Trough margin. Sedimentology 57, 912–931.

Wadge, G., Voight, B., Sparks, R.S.J., Cole, P., Loughlin, S.C., 2014. An overview of the eruption of Soufrière Hills Volcano from 2000-2010. In: The Eruption of the Soufrière Hills Volcano, Montserrat from 2000-2010 edited by Wadge, G., Robertson, R.A.E. and Voight, B. Geological Society Memoir 39, 1-40.

955 Watt, S.F.L., Talling, P.J., Vardy, M.E., Masson, D.G., Henstock, T.J., Hühnerbach, V.,
956 Minshull, T.A., Urlaub, M., Lebas, E., Le Friant, A., Berndt, C., Crutchley, G.J., Karstens, J.,
957 2012. Widespread and progressive seafloor-sediment failure following volcanic debris
958 avalanche emplacement: landslide dynamics and timing offshore Montserrat, Lesser Antilles.
959 Mar. Geol. 323–325, 69–94. https//doi:10.1016/ j.margeo.2012.08.002
960
961 Watt, S.F.L., Jutzeler, M., Talling, P.J., Carey, S.N., Sparks, R.S.J., Tucker, M.E, Stinton,
962 A.J., Fisher, J.K., Wall- Palmer, D., Hühnerbach, V., Moreton, S.G., 2015. New insights into
963 landslide processes around volcanic islands from Remotely Operated Vehicle (ROV)
964 observations offshore Montserrat. Geochemistry, Geophysics, Geosystems 16, 2240-2261.
965
966 Whitaker, F.F., Smart, P.L., 1990. Active circulation of saline ground waters
967 in carbonate platforms: Evidence from the Great Bahama Bank. Geology 18,
968 200-203.
969
970 Zellmer, G.F., Hawkesworth, C.J., Sparks, R.S.J., Thomas, L.E., Harford,
971 C.L., Brewer, T.S., Loughlin, S.C., 2003. Geochemical evolution of the
972 Soufrière Hills Volcano, Montserrat, Lesser Antilles Volcanic Arc. Journal of
973 Petrology 44, 1349-1374.
974
975
976 **Captions to figures**
977
978 Fig. 1. Map showing the location of Montserrat island in the northern Lesser Antilles and the
979 bathymetry of the surrounding seafloor. Principal volcanic centers on Montserrat are marked

by red triangles. Faults are indicated based on Feuillet et al. (2010) and on interpretation of seismic reflection data in Watt et al. (2012). The inset map shows the location of the study region within the Lesser Antilles. Locations of seismic reflection lines from previous studies are indicated by the blue and green lines that cross the Kahouanne valley.

Fig. 2. Maps showing the location of carbonate samples from a) Kick'em Jenny submarine volcano area in the southern Lesser Antilles and b) Kolumbo submarine volcano and other seamounts northeast of the Santorini volcanic complex in the southern Aegean Sea. Sample localities are shown with red stars. Insert map in the Kolumbo figure shows the location of the sampling area relative to Santorini.

Fig. 3. High-resolution multibeam map of the area southeast, south, and east of the island of Montserrat. Carbonate samples used in the study are shown by red stars. Depth key is in the lower right-hand corner of the figure. Irregular hummocky seafloor to the south and east of Montserrat consists of large-scale debris avalanche deposits.

Fig. 4. Montserrat SW Nearshore. a) Collecting sample NA037-029 at 188 m depth from low cliff. b) Well-indurated volcaniclastic-bioclastic pack-grain-rudstone with volcanic clasts coated by coralline algae. c) Micrite-filled sponge borings cutting shell and adjacent sediment indicating 2 phases cementation (thin-section, ppl). d) Grains cemented by isopachous fibrous calcite crust (thin-section, ppl).

Fig. 5. Montserrat SW Nearshore. a) Site of sample NA037-033 at 292 m. b) Cemented slope sediment consisting of volcanic clasts encrusted with calcareous algae, in a bioclastic

volcaniclastic pack-grain-rudstone with shell fragments. c) Encrustation of volcanic clast with foraminifera, serpulids and calcareous red algae (thin-section, ppl). d) Peloids between grains, probably microbial (thin-section, ppl). e) Volcanic and bioclastic grains cemented by isopachous calcite fringe (thin-section, xp). f) Isopachous calcite cement fringe around bioclasts (thin-section, ppl).

Fig. 6. Montserrat SW Offshore, sample NA037-025, depth 806 m. a) Cemented bioclastic-volcaniclastic grainstone. b) Bioclasts, intragranular peloidal sediment, fringing calcite cement (thin-section, ppl). c) Isopachous fibrous calcite cement around grains (thin-section, ppl). d) SEM-BSE micrograph of calcite cement around bioclasts and aragonite cement within gastropod (upper left).

Fig. 7. Montserrat SW Offshore. a) Collecting sample NA037-026, depth 823 m. b), c) Bioclastic-volcanic pack-grain-rudstone with bio-coated volcanic grains (thin-section, ppl). d) Encrustation of volcanic clast by foraminifera, coralline algae, microbialite with filaments and serpulid (thin-section, ppl). e) Gastropod shell (formerly aragonite) dissolved out; whorl filled with calcite spar cement (thin-section, ppl).

Fig. 8. Kick'em Jenny, off Grenada. a) Sampling the seafloor crust. b) Sample NA039-071, 1956 m depth. Pelagic lime mudstone with large burrows. c) Intraclasts and pellets of lime mud within burrow cavity. Patchy calcite cement fringes around clasts (thin-section, ppl). d) Ostracod filled by microfossiliferous lime mud; patchy bladed-fibrous calcite cement around shells (thin-section, ppl).

1028 Fig. 9. Kick'em Jenny sample NA039-035, depth 172 m. a) Volcaniclastic material with
1029 patches of dark lime mud, some of which may have infiltrated cavities. Note cavities filled
1030 with peloids (thin-section, ppl). b) Close-up of micritic peloids, probably of microbial origin,
1031 within cavities (thin-section, ppl).

1032

1033 Fig. 10. Kolumbo seamount. a) Sample NA007-001 depth 200 m – a pelagic limestone with
1034 fine volcanic material, with 2 phases of sponge boring, 2nd phase empty, and bivalve shell
1035 (thin-section, ppl). b) Collecting sample NA007-022, depth 194 m, with several crust layers.
1036 c), d) NA007-022 A complex volcaniclastic limestone calcareous alga with cavities (likely
1037 sponge borings) lined by a thin calcite cement crust, followed by an influx of pelagic
1038 sediment. Empty sponge borings from a later phase of boring (thin-section, ppl).

1039

1040 Fig. 11. Kolumbo seamount. a) Collecting sample NA007-045, depth 128 m. b), c), d) Loose
1041 coralline red algal framework with fine volcaniclastic-bioclastic material partly filling growth
1042 cavities. (b), c) thin-section, ppl; d) (xp).

1043

1044 Fig. 12. Carbon and oxygen isotope cross-plot (‰ VPDB) for crust samples and for samples
1045 from the geothermal well Mon3 and Roche's Bluff. Sample names are given on the figure for
1046 values plotting outside the marine area (i.e. positive $\delta^{18}O$ and $\delta^{13}C$). Also shown are the
1047 positions of the $\delta^{18}O$ values (but ‰ VSMOW) for geothermal and spring water from
1048 Hemmings et al. (2015) and Chiodini et al. (1996) respectively, and for fresh and altered
1049 SHV andesite from Zellmer et al. (2003).

1050

1051 Fig 13. Schematic model for formation of slope crusts on a seamount developed through

precipitation of carbonate from seawater entering the volcanic edifice through ocean currents, waves and storms, and seawater drawn in through Kohout convection.

Figure 1

Fig. 1

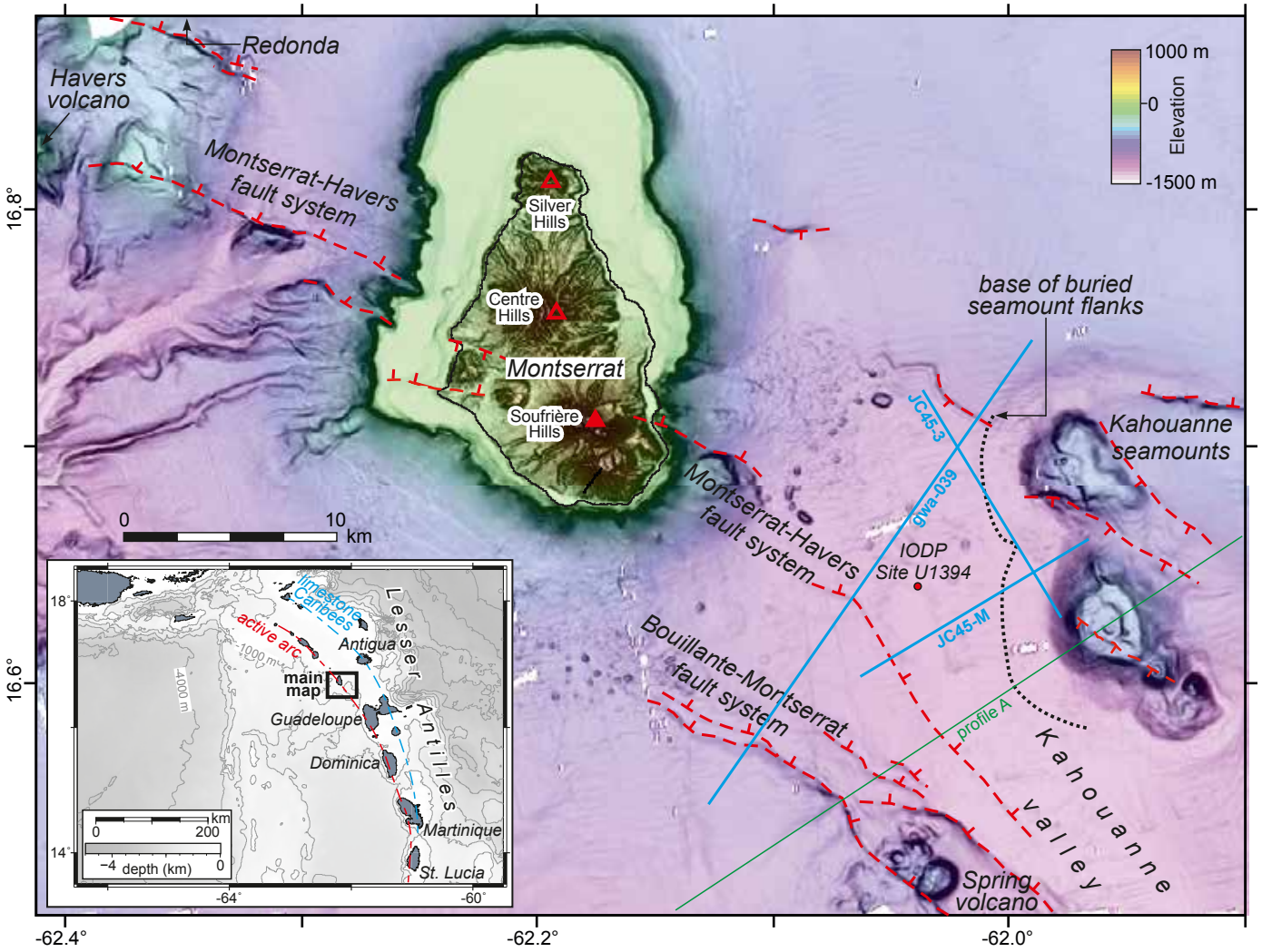

A.

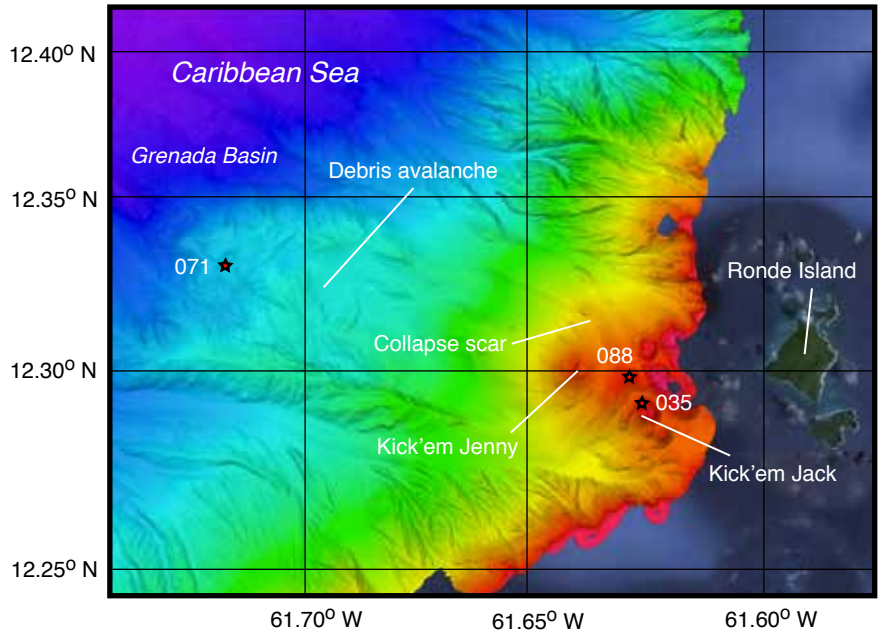
12.40° N
12.35° N
12.30° N
12.25° N
61.70° W
61.65° W
61.60° W
Caribbean Sea
Grenada Basin
Debris avalanche
071
Ronde Island
Collapse scar
088
035
Kick'em Jenny
Kick'em Jack

B.

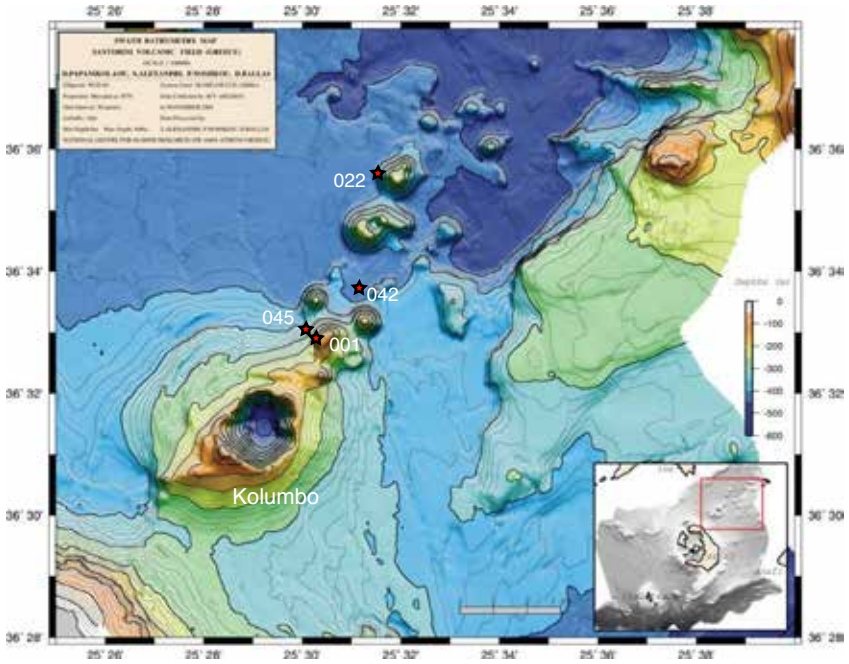
022
042
045
001
Kolumbo

Figure 3

Fig. 3

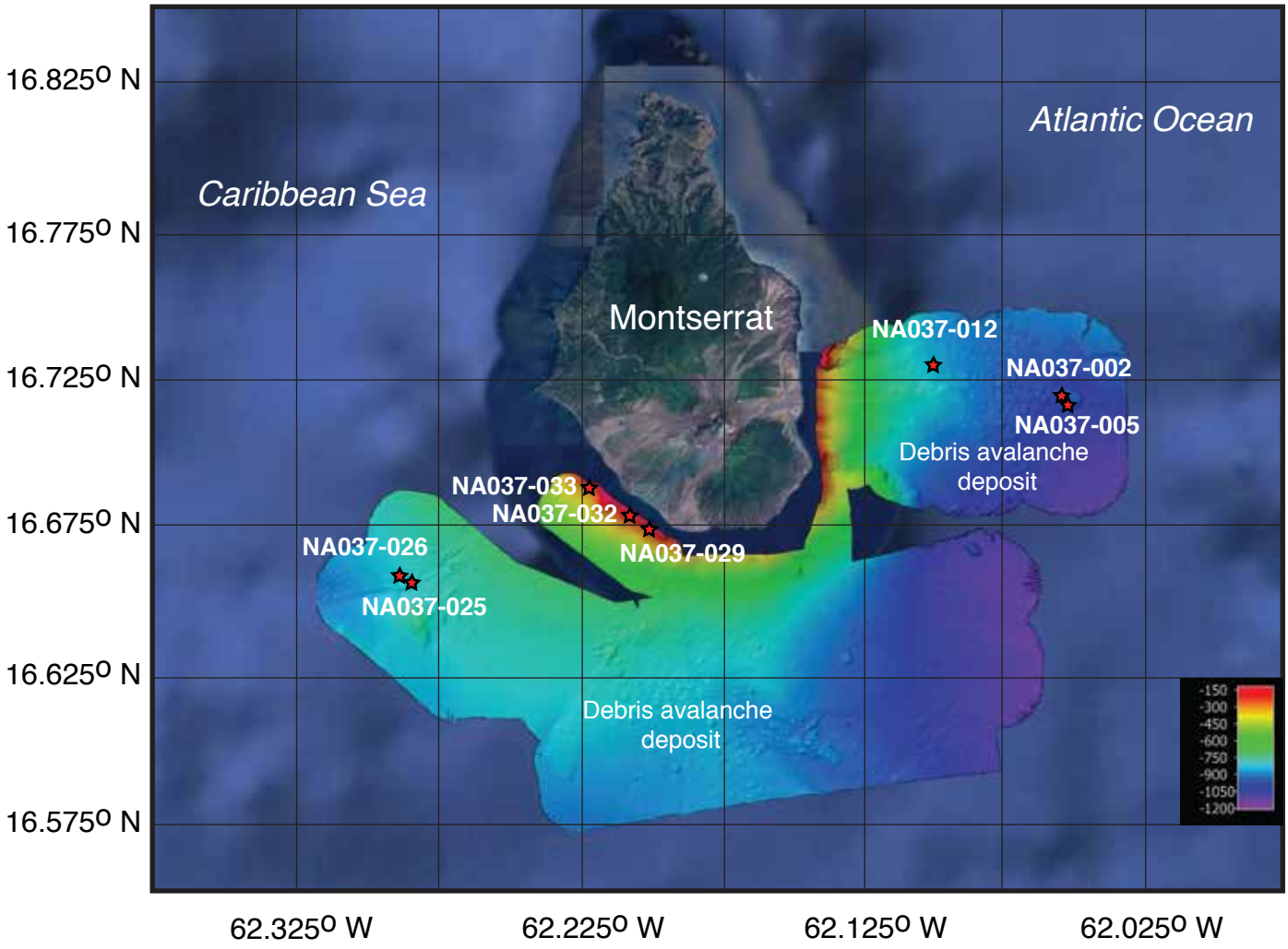

Figure 4

Fig. 4

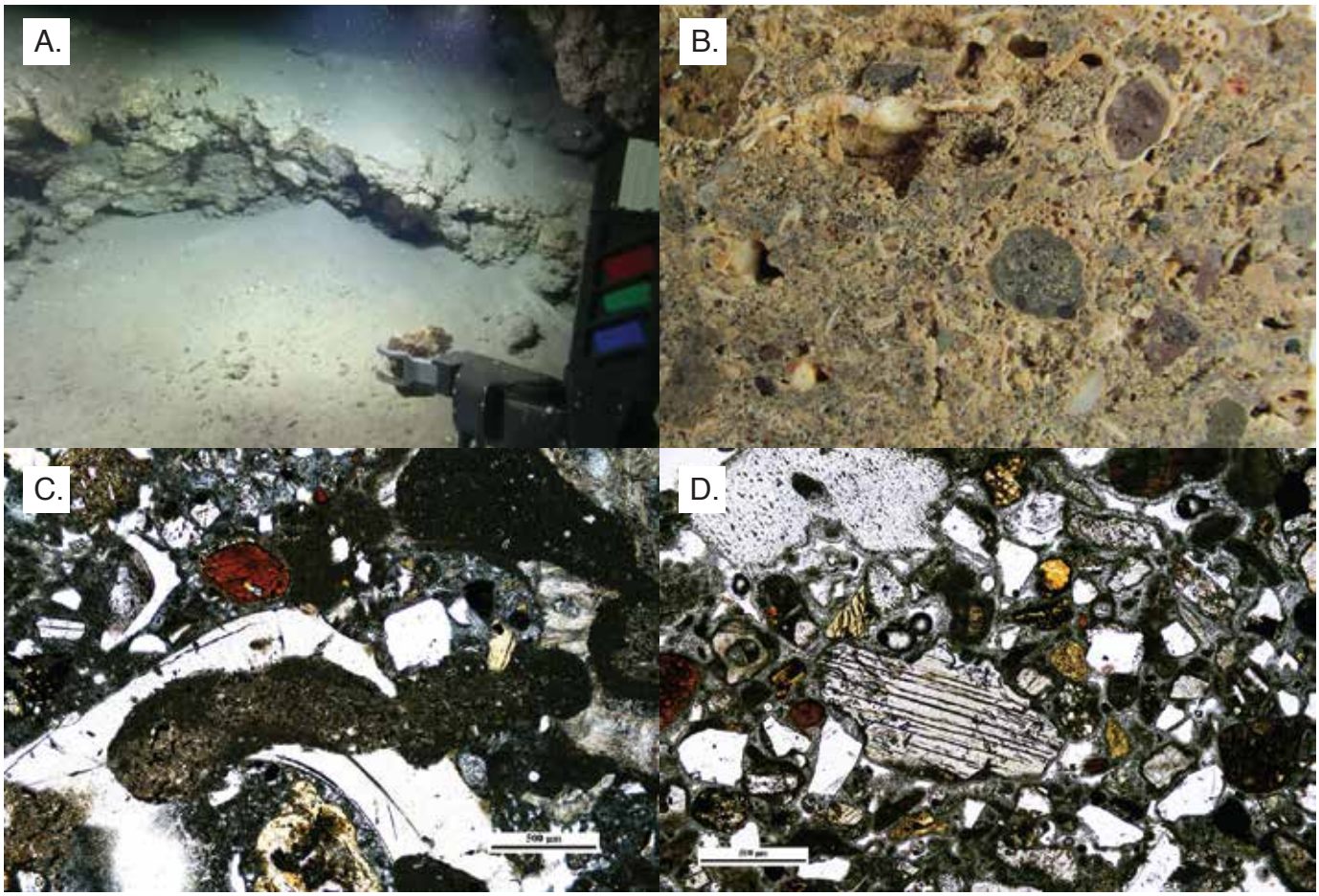

Figure 5

Fig. 5

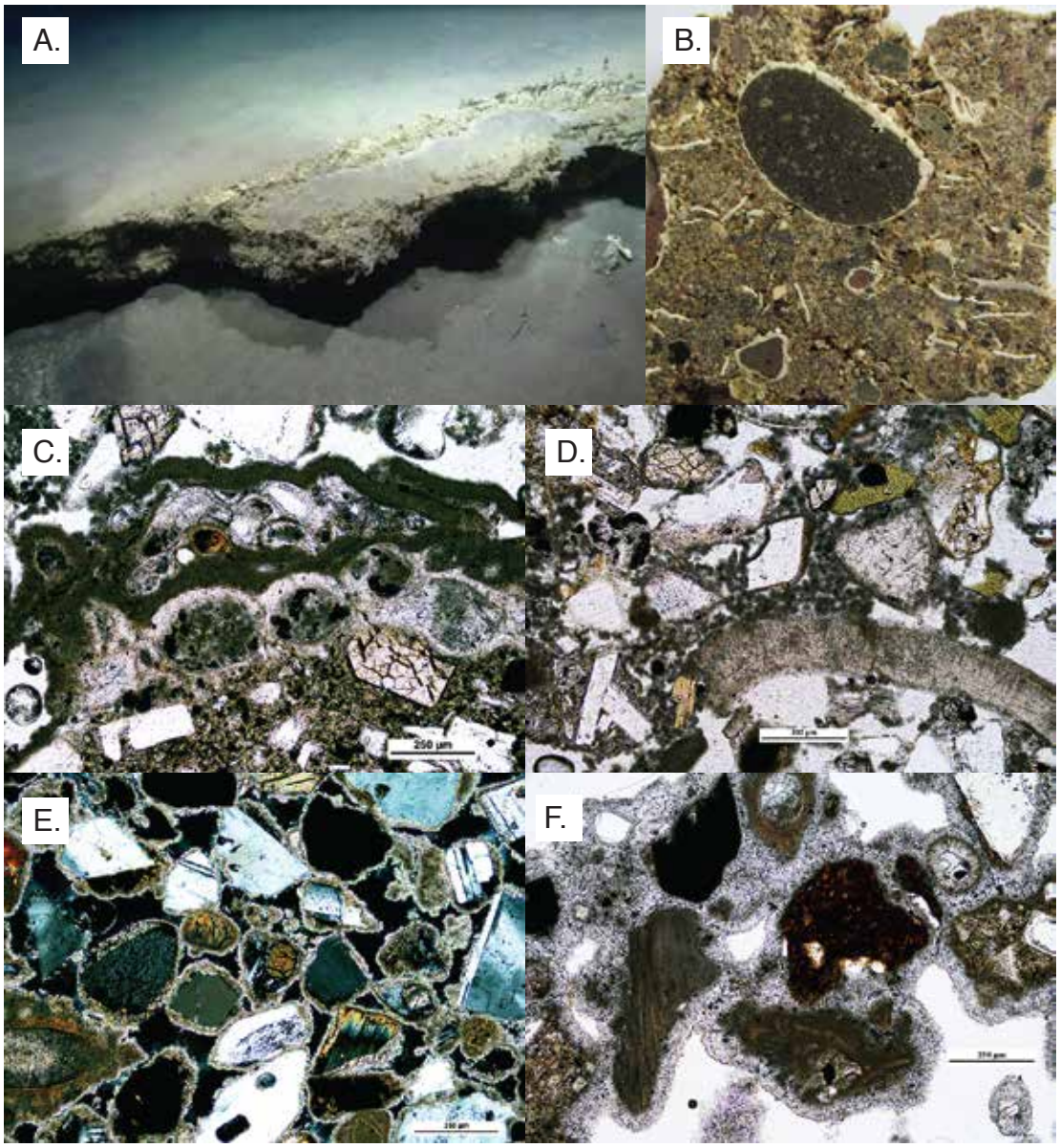

Figure 6

Fig. 6

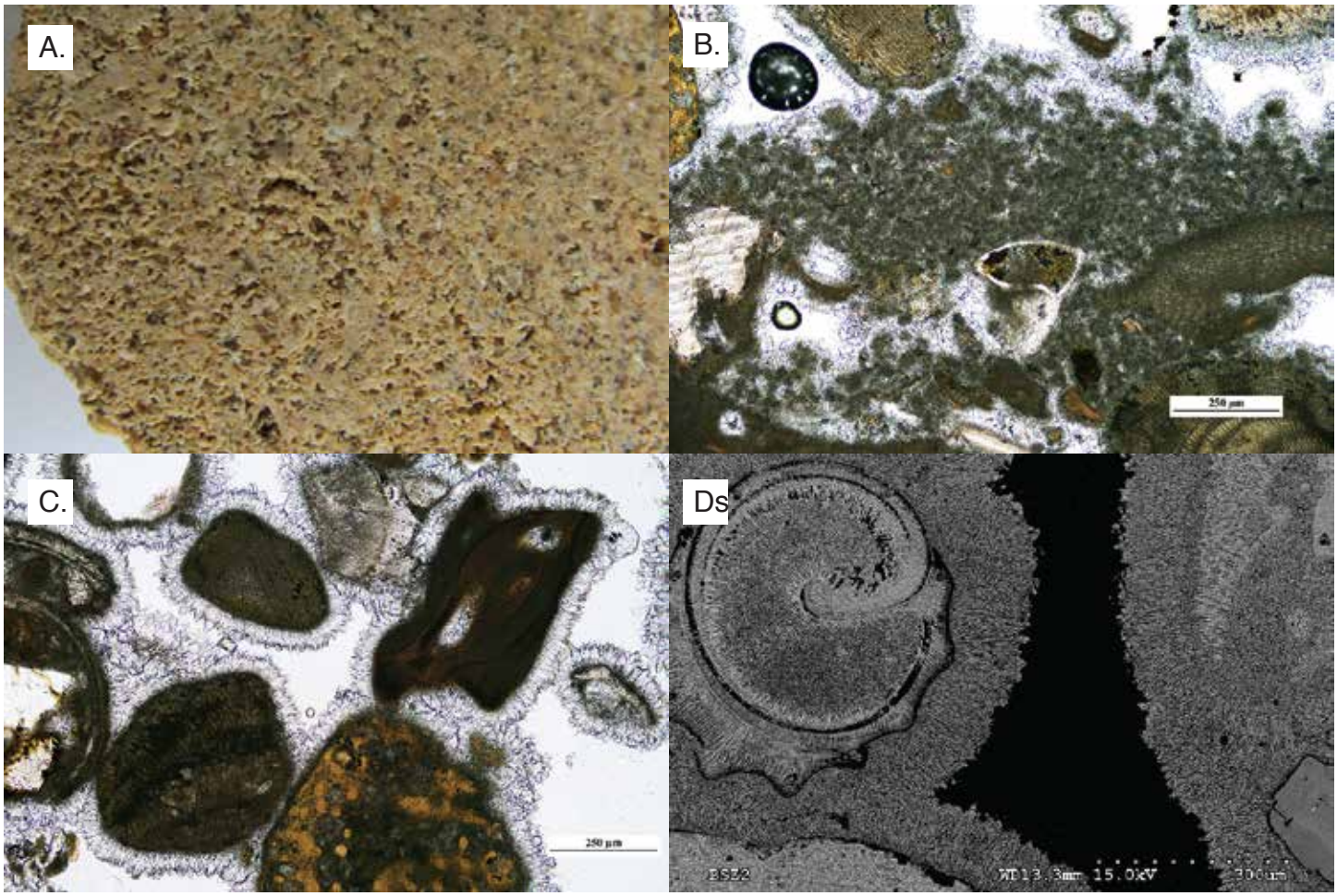

Figure 7

Fig. 7

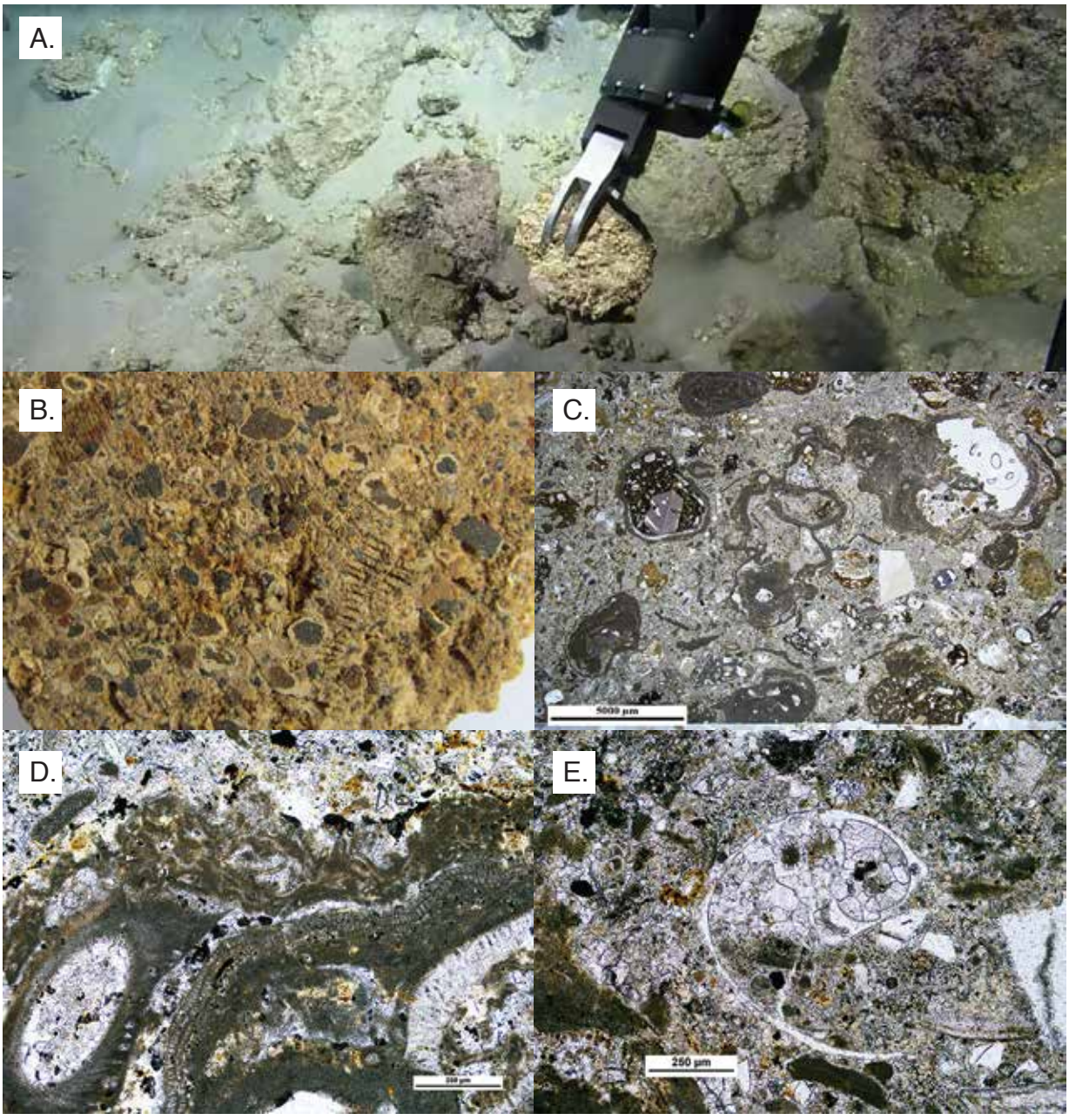

Figure 8

Fig. 8

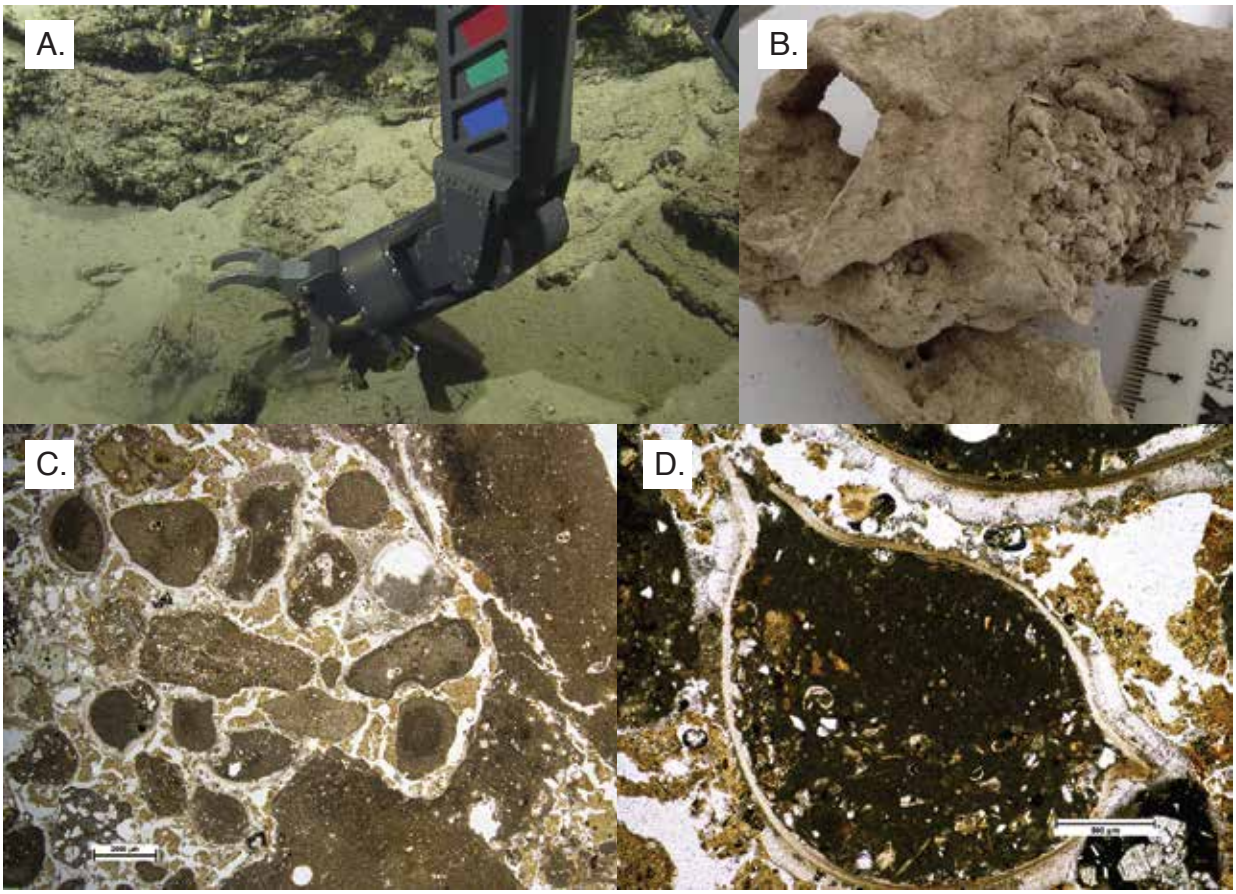

Figure 9

Fig. 9

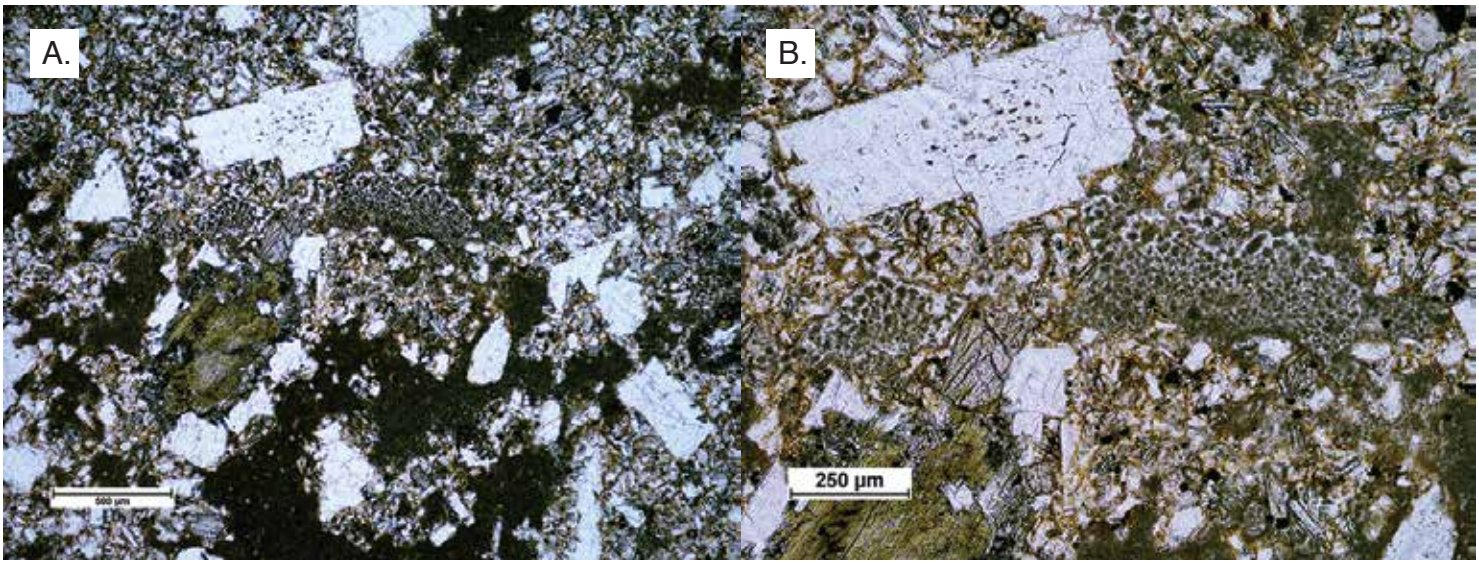

Figure 10

Fig. 10

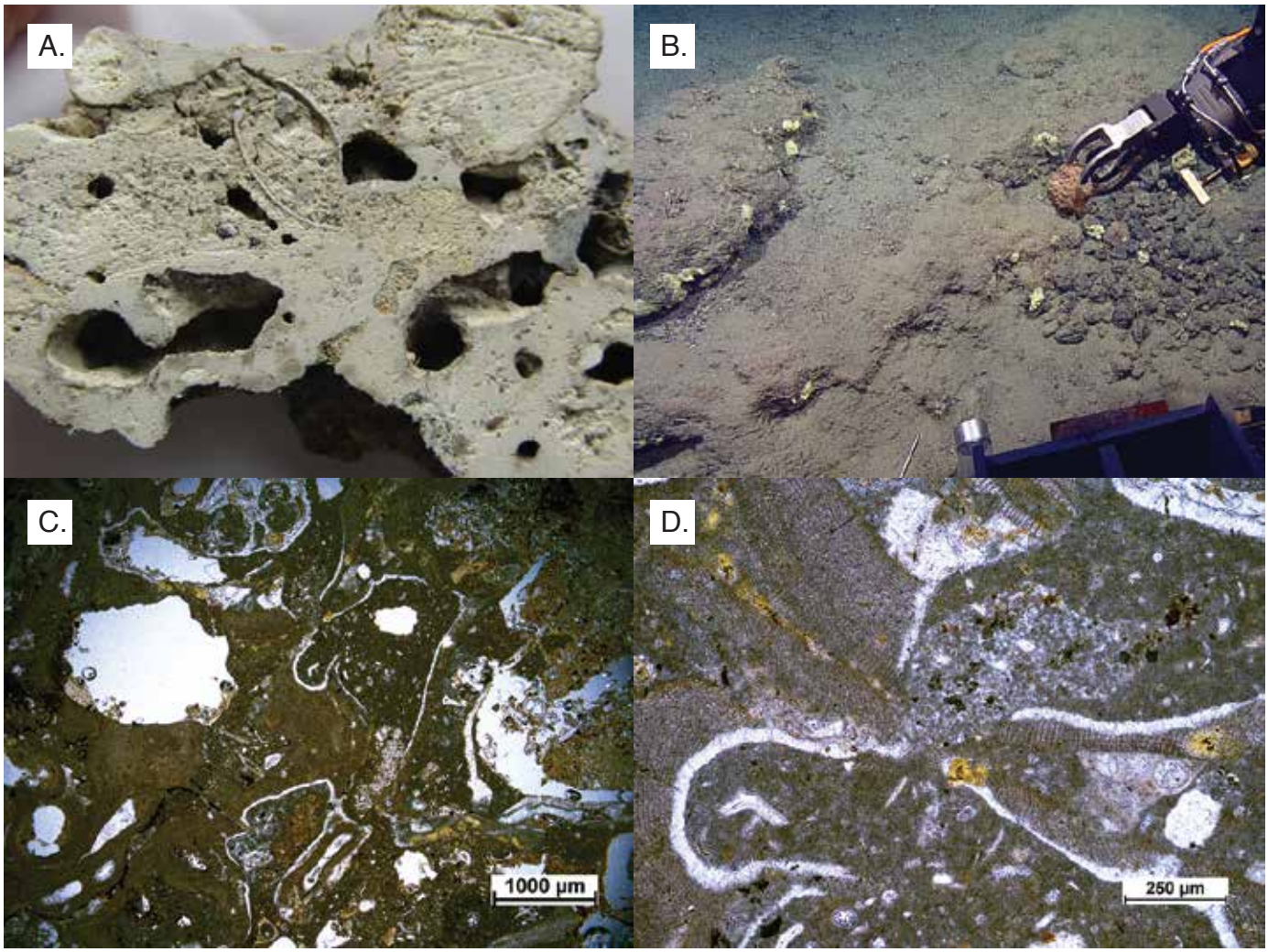

Figure 11

Fig. 11

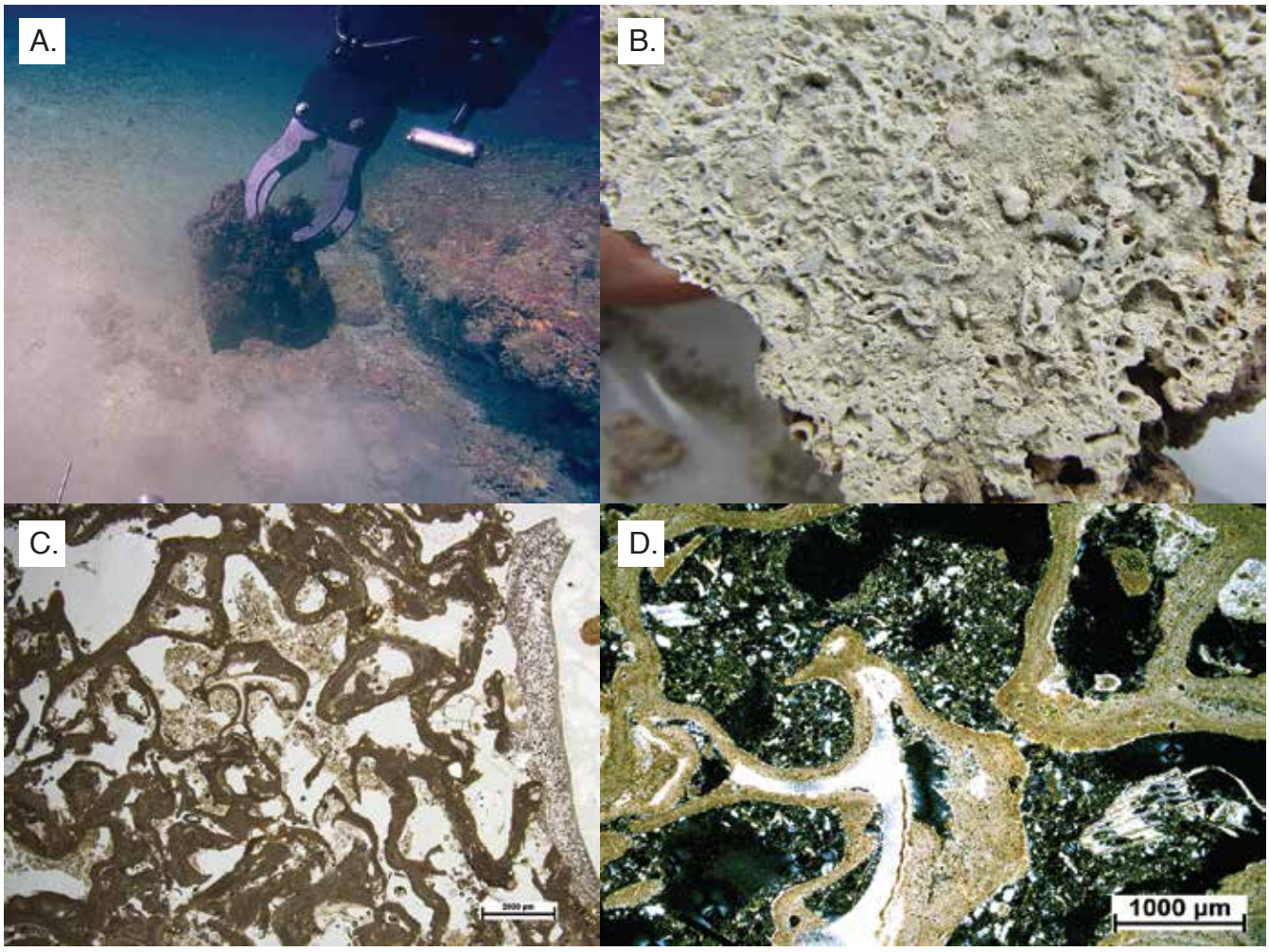

Figure 12

Fig. 12

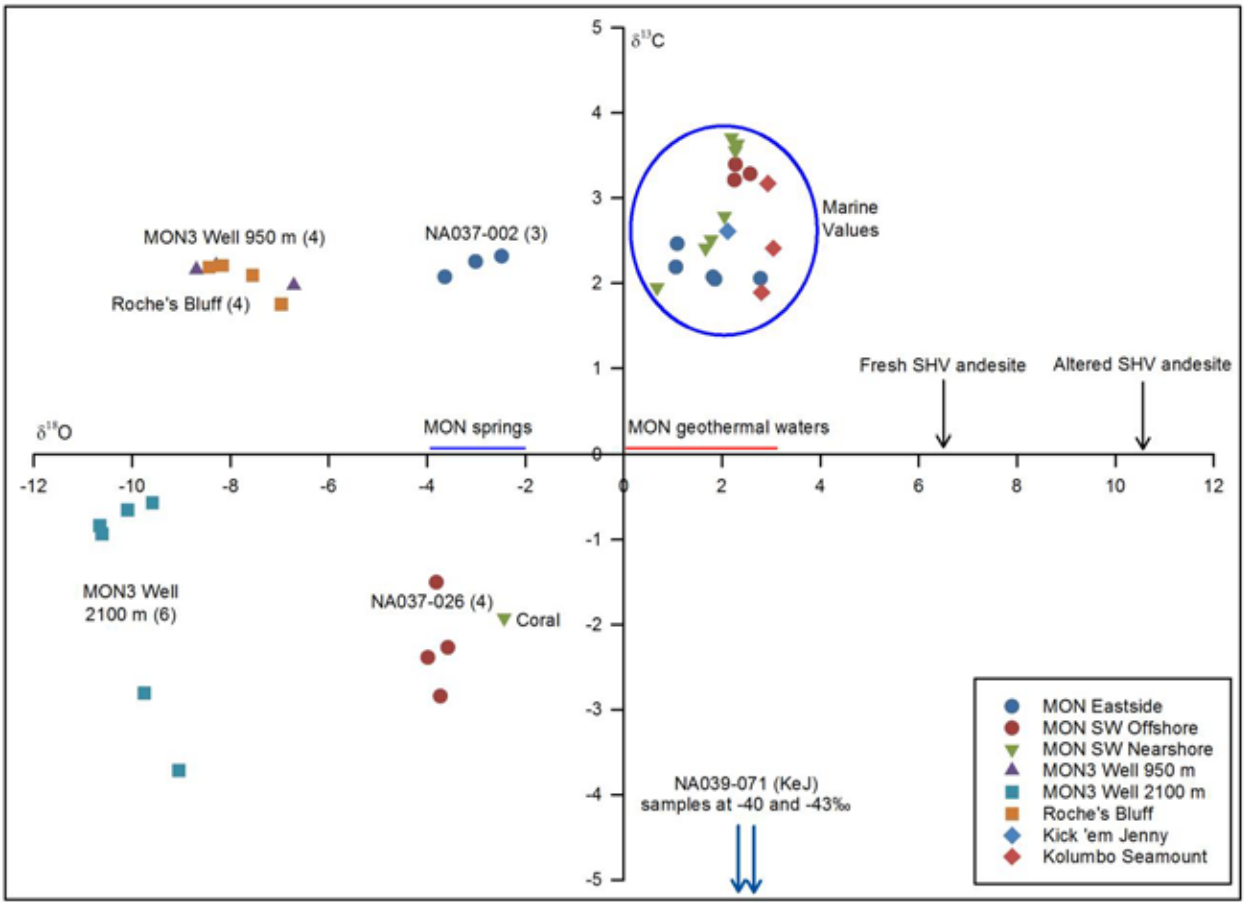

Figure 13

Fig. 13

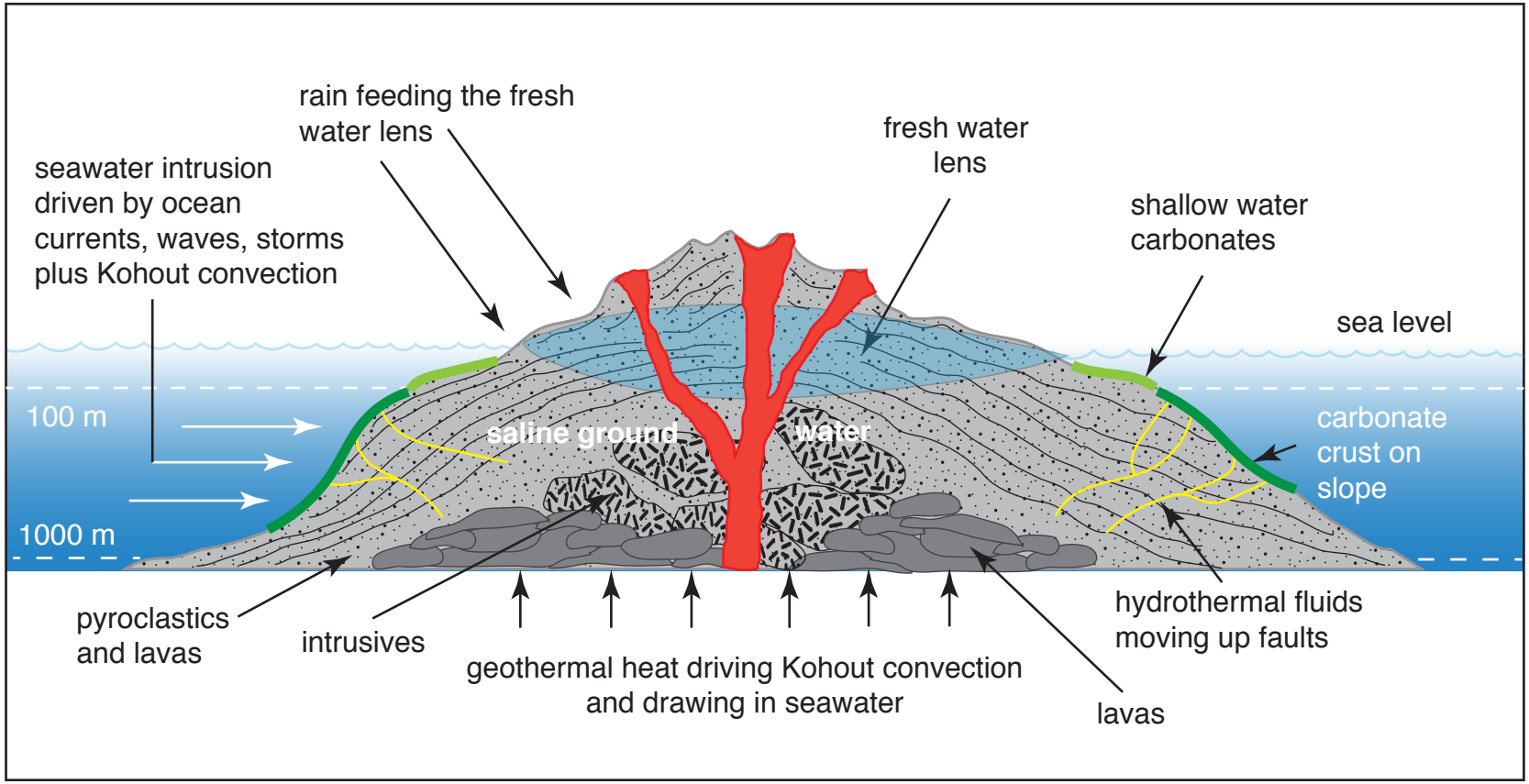

table 1

Click here to access/download

Table

Table01.pdf

Table 2

Table 3

Click here to access/download

Table

Table03.pdf

Conflicts of Interests

None of the authors has any financial or personal relationships with other people or organizations that could inappropriately influence their work.